MIKE
Powered by **DHI**

MOUSE

Pipe Flow

Reference Manual

PLEASE NOTE

COPYRIGHT

This document refers to proprietary computer software which is protected by copyright. All rights are reserved. Copying or other reproduction of this manual or the related programs is prohibited without prior written consent of DHI. For details please refer to your 'DHI Software Licence Agreement'.

LIMITED LIABILITY

The liability of DHI is limited as specified in your DHI Software Licence Agreement:

In no event shall DHI or its representatives (agents and suppliers) be liable for any damages whatsoever including, without limitation, special, indirect, incidental or consequential damages or damages for loss of business profits or savings, business interruption, loss of business information or other pecuniary loss arising in connection with the Agreement, e.g. out of Licensee's use of or the inability to use the Software, even if DHI has been advised of the possibility of such damages.

This limitation shall apply to claims of personal injury to the extent permitted by law. Some jurisdictions do not allow the exclusion or limitation of liability for consequential, special, indirect, incidental damages and, accordingly, some portions of these limitations may not apply.

Notwithstanding the above, DHI's total liability (whether in contract, tort, including negligence, or otherwise) under or in connection with the Agreement shall in aggregate during the term not exceed the lesser of EUR 10.000 or the fees paid by Licensee under the Agreement during the 12 months' period previous to the event giving rise to a claim.

Licensee acknowledge that the liability limitations and exclusions set out in the Agreement reflect the allocation of risk negotiated and agreed by the parties and that DHI would not enter into the Agreement without these limitations and exclusions on its liability. These limitations and exclusions will apply notwithstanding any failure of essential purpose of any limited remedy.

CONTENTS

MOUSE PIPE FLOW

Reference Manual

1   A General Description

The MOUSE Pipe Flow Model is a computational tool for simulations of unsteady flows in pipe networks with alternating free surface and pressurised flow conditions. The computation is based on an implicit, finite difference numerical solution of basic 1-D, free surface flow equations (Saint Venant). The implemented algorithm provides efficient and accurate solutions in multiply connected branched and looped pipe networks.

The computational scheme is applicable to vertically homogeneous flow conditions which occur in pipes ranging from small-profile collectors for detailed urban drainage, to low-lying, often pressurised sewer mains, affected by the varying water level at the outlet. Hydrodynamics of prismatic open channels can also be simulated.

Both sub-critical and supercritical flows are treated by means of the same numerical scheme that adapts according to the local flow conditions. Naturally, flow features such as backwater effects and surcharges are precisely simulated.

Pressurised flow computations are facilitated through implementation of a narrow 'slot', as a vertical extension of a closed pipe cross section. Free surface and pressurised flows are thus described within the same basic algorithm, which ensures a smooth and stable transition between the two flow types.

The complete non-linear flow equations can be solved for user-specified or automatically supplied boundary conditions. In addition to this fully dynamic description, simplified flow descriptions are available.

Within the Pipe Flow Model, advanced computational formulations enable description of a variety of pipe network elements, system operation features and flow phenomena, e.g.:

- flexible cross-section database, including standard shapes;
- circular manholes;
- detention basins;
- overflow weirs;
- pump operation;
- passive and active flow regulation;
- constant or time variable outlet water level;
- constant or time variable inflows into the sewer network;
- head losses at manholes and basins;
- depth-variable friction coefficients.

The features implemented in conceptualisation of the physical system and the flow process enable realistic and reliable simulations of the performance of both existing sewer systems and those under design.

2 Modelling the Physical System

2.1 The Model Elements - Inventory

Elements available for definition of a numerical model in MOUSE are:

1. Links

- pipes - standard and arbitrary cross-sections,
- open channels - arbitrary cross-sections.

2. Nodes

- manholes,
- basins (structures),
- storage nodes,
- outlets.

3. Functions, for description of certain physical components of sewer systems, including:

- overflow weirs,
- orifices,
- pumps,
- non-return valves,
- flow regulators.

4. Controllable structures, for the simulation of reactive or time dependent operation real-time control, including:

- rectangular underflow gate with movable blade,
- rectangular overflow weir with changeable crest elevation.

Principles underlying the concept of controllable structures are described in the "MIKE URBAN Collection System User Guide".

2.2 Links

2.2.1 General Description

Links in MOUSE Pipe Flow Model are defined as one-dimensional water conduits, connecting two nodes in the model. The link definition allows that the dependent flow variables (e.g. water levels and discharges) can be uniquely described as functions of time and space.

A link is featured by constant cross-section geometry, constant bottom slope and constant friction properties along the entire length. A straight layout is assumed.

MOUSE supports two classes of links:

- closed conduit links (pipes),
- open channel links.

Closed conduits under certain hydraulic conditions may become pressurised. In such a case, the confinement of the flow fundamentally changes the environment in which the flow process takes place, but the MOUSE Pipe Flow Model continues to perform the computations using the same flow description as for open channel flow. This is possible, because MOUSE furnishes actually closed conduits (pipes) with a fictitious slot (Preissmann slot) on the top of the cross section, thus replacing a pipe with an open channel, featuring a cross section shaped to approximate the hydraulic behaviour of a pressurised pipe.

2.2.2 Specification of a Link

Specification of a Link requires specification of the associated nodes (see paragraph *2.3 Nodes (p. 19)*), the link material, longitudinal parameters and the cross-section definition (shape and size).

Link Material

The parameter which characterises the link material is the link friction, expressed as Manning's number (*M* or *n = 1/M*). The link can be defined as

constituted of one of 8 predefined material types. Table 2.1 lists the available link materials with MOUSE default values for Manning's number.

Table 2.1   Manning's Numbers - MOUSE Default Values

MOUSE Code	Material	Mouse M	Default Value N=1/M
1	Smooth Concrete	85	0.0118
2	Normal Concrete	75	0.0133
3	Rough Concrete	68	0.0147
4	Plastic	80	0.0125
5	Iron	70	0.0143
6	Ceramics	70	0.0143
7	Stone	80	0.0125
8	Other	50	0.0200

Fig 0.0.1

The default values can be edited by the user. The modified default values are associated with the current project only; i.e. will affect any simulation carried out with the MOUSE project file. Also, the default Manning number for any individual link can be overwritten by a user-specified, link-specific value.

Longitudinal Profile

A link is longitudinally defined by bottom elevations of the upstream and downstream end. By default, link bottom elevations are assumed to be equal to the adjacent node's bottom elevations. The default setting can be over-ruled by specification of the actual link end elevations, but not below the node bottom.

Normally, length of a link is calculated on the basis of the nodes co-ordinates. The length computation will take into account if the link between the nodes is not straight. Optionally, for links connected to circular manholes, it is possible to calculate the length from the manhole perimeter.

In cases where actual link length significantly deviates from the calculated value, a user-specified length can be supplied instead.

Longitudinal slope of a link is assumed constant. It is calculated using link end elevations and the link length.

Specification of a node as "upstream" or "downstream" has, in principle, only a declarative meaning and does not affect the computations. An exception is if the functions located in the link (see sections 2.4.2 Orifice Function *(p. 30)*, 2.4.3 Pump Function *(p. 44)* and 2.4.4 Flow Regulation *(p. 45))* are present in the model. In the flow regulation (restriction), only positive flow is affected by the regulation. Similarly, the non-return valve function allows only positive flow.

By convention, positive flow values represent the flow in the direction from "upstream" to "downstream" node.

Link Cross-Sections

As a built-in feature, MOUSE supports four different pipe cross-section types. Any other "non-standard" pipe, tunnel or open channel can be described through the Cross-section database facility (by specifying the geometric shape of the cross section or a table of geometrical parameters.

MOUSE includes the following standard pipes:

1. Circular pipe,
2. Rectangular pipe (B ≠ H),
3. O-shaped pipe (H/B = 1.125/1),
4. Egg-shaped pipe (H/B = 1.5/1),
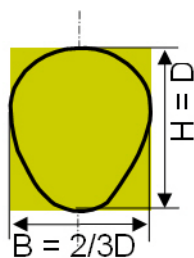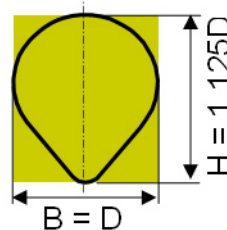
Figure 2.1 MOUSE egg-shaped cross-sections. Note the difference in selection of the characteristic dimension D.

Any of the four "standard" pipe cross sections is fully defined by specifying the pipe type, and characteristic dimension(s). While for the circular and rectangular shape, this is straightforward, attention should be paid for the definition of the egg-shaped cross sections. For the O-shaped pipe the dimension to be specified is the width (D, [m]), and for the Egg-shaped pipe the dimension to be specified is the cross-section height.

The non-standard link cross-sections can be specified and maintained through the Cross-section Editor. Cross-sections are distinguished as "opened" and "closed", i.e. open channels on the one side, and pipes and tunnels on the other.

The data required for description of a non-standard cross-section can be entered in a raw form, either in a X-Z or in Height-Width format (please refer to the user guide), which gives six options in total.
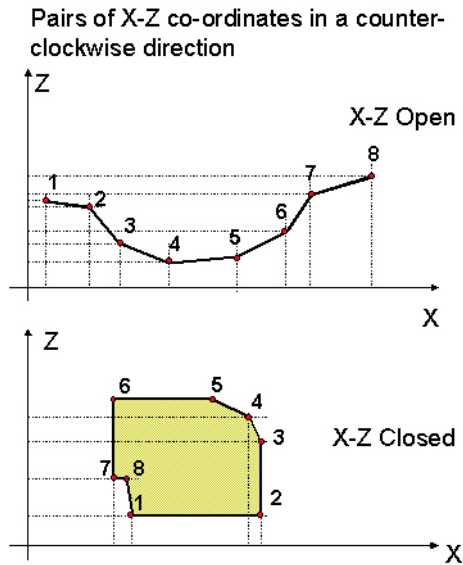
Figure 2.2   X-Z types of cross-sections
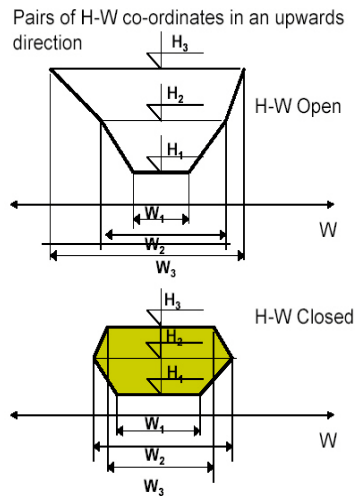
Figure 2.3   H-W types of Cross-sections

The raw geometrical data are then automatically processed, in order to create tables with parameters suitable for flow computations. Such a table contains 50 data sets, covering the range from the lowest to the highest point specified, in equal increments.

The parameters in the table are:

W	=	surface width, [m]
L	=	height (relative depth), [m]
A	=	cross-section area, [m^2]
R	= A/P =	hydraulic radius, [m]

In case of a closed link, MOUSE automatically provides an appropriate slot for pressurised flow computations, see section 3.3 Modelling The Pressurised Flow *(p. 54)*.

Intermediate values are linearly interpolated.

The first set of values is associated with depth equal to zero ($y = 0$), and the last set with the maximum specified value (relative to the bottom).

For open channels, MOUSE will compute the flow as long as the water level is below the lower end of the cross-section. If this level is exceeded, the computation will be stopped unless extrapolation of cross-section is specified in the DHIAPP.INI file. For closed conduits, MOUSE allows an unlimited raise of pressure; i.e. Preissmann slot is extended indefinitely in the height.

Processed data for a cross section is specified as a table with depth (Y), width (B), area (A) and hydraulic radius (R). Conveyance is computed automatically by MOUSE as *C = AR2/3*.

The processed cross-section data table for an open cross-section should cover the whole range of the expected oscillation of the water surface. If the water surface exceeds the maximum specified elevation in the table, the computation is stopped.

For closed cross-sections, the processed data table has to cover the entire range from the bottom to the top of the cross-section. MOUSE adds the Preissmann slot (see ref. /4/) automatically.

To ensure the computational stability, the cross-section conveyance should be maintained monotonously increasing (or at least constant) with increase of water level. This is normally not the case with closed conduits, where the value of conveyance drops in the region near the top of the section. For such cases, when raw data are input, MOUSE adjusts the hydraulic radius so that the limiting conveyance for the cross-section corresponds to the actual conveyance value for the full profile. When closed cross-section data are input in the processed form, attention should be paid in the upper region of the profile, so that decreasing conveyance is avoided.

2.3 Nodes

2.3.1 General Description

Points associated with link ends and junctions are called nodes. Each link is actually defined with exactly two nodes. Depending on the position in a network layout, a node is associated with one or more links. In the later case, a node is called a junction. An arbitrary number of links can be attached to a junction, thus allowing construction of arbitrary network layouts.

2.3.2 Types and Definition of Nodes

Every node in a network is defined by its identification (max. 25 characters) and its *x* and *y* co-ordinates, [m]. Exception is storage nodes, which do not require co-ordinates. Further, according to the type of node, an appropriate set of parameters is required.

Circular Manholes

Circular manhole is a vertical cylinder, defined by the following parameters:

H_{bott}	=	bottom elevation, [m]
H_{top}	=	surface elevation, [m]
D_m	=	diameter, [m]
K	=	outlet shape, types 1-9

Definition of the outlet shape is connected with calculation of head losses in nodes (see section 7.2 Head Losses in Manholes and Structures - Introduction *(p. 88)*).

MANHOLE DATA:

X-coordinate
Y-coordinate
Diameter [m]
Ground Level [mabs.]
Invert Level [mabs.]
Critical Level [mabs.]
Outlet Shape
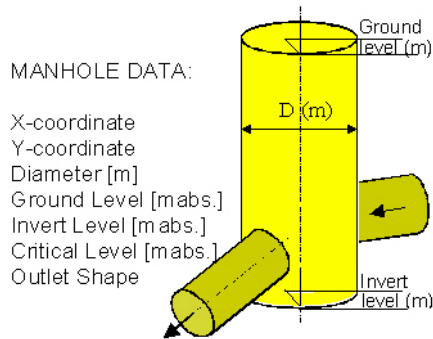
Figure 2.4   MOUSE manhole

Flow conditions in a manhole are an important element of the overall flow description. The following parameters are calculated:

H_m=water level in a manhole, [m]

v_m=   velocity, calculated per default as:

$$v_m = \frac{Q}{(H_m - H_{bott}) \cdot D_m}$$

(2.1)

i.e. uniform velocity distribution is assumed.

The flow area calculated as above gives a very conservatively low estimate of the velocity head and hence a conservative energy loss in the manhole, causing higher water levels in the manholes than observed in reality.

An alternative formula for a more realistic calculation of the flow area in manholes is also available – however only for "flow-through" manholes with one inlet pipe and one outlet pipe. The alternative formulation is based on the assumption that the inflow behaves like a submerged jet, which entrains water from the ambient fluid and increases the discharge through the manhole. The angle of entrainment is approximately 6.8°. The cross-section area of the jet thus depends on the distance from the inlet.

As a generalisation, it is assumed that the effective flow area in the manhole equals the cross-section area of the jet at the outlet. This is valid in the case of no change in direction from inlet to outlet. It is calculated as:

$$A_{flow}= A_{jet} = \frac{\pi}{4} \cdot D_{in}^2 \cdot \left(1 + 2 \cdot \frac{D_m}{D_{in}} \cdot \tan\left(\frac{6.8}{360} \cdot 2\pi\right)\right)^2$$

(2.2)

where D_{in} is the diameter of the inlet pipe.

So far, the alternative formula is only applicable in MOUSE for manholes with one inlet and one outlet. However, the implementation includes the possibility for a change in elevation and a change in flow direction from inlet to outlet.
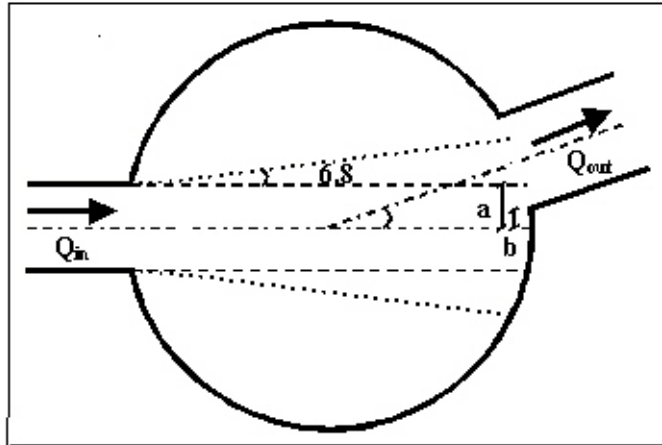
Figure 2.5   Manhole with one inlet, one outlet and a change in flow direction.

In the case of a change in flow direction the effect of the jet at the outlet will gradually diminish with increasing angle. The effective flow area is therefore linearly interpolated between the full cross-section area of the manhole, A_m, and the area of the jet, A_{jet}, as the angle increases.

The distance, a, from the point where the jet intercepts the manhole to the centreline of the inlet, see Figure 2.5, is conservatively calculated as half the diameter of the inlet, D_{in}, thus neglecting the entrainment angle of 6.8°.

$$a = \frac{D_{in}}{2} \tag{2.3}$$

The distance, b, from the point where the side of the outlet enters the manhole to the centreline of the inlet is approximated with

$$b = \frac{D_m}{2} \cdot \tan\left(\frac{\theta}{360} \cdot 2\pi\right) - \frac{D_{out}}{2} \tag{2.4}$$

where θ is the angle between the centrelines of the inlet/outlet and D_{out} is the diameter of the outlet pipe.

In the case of a change in elevation the effective flow area is diminished with a factor, *drop_factor*, which is equal to 1 when the inlet flows directly into the outlet and 0 when there is no interception between the incoming jet (calculated conservatively without the entrainment angle) and the outlet. In between these two conditions the drop factor is interpolated linearly.

The effective flow area is then interpolated as:

$$A_{flow} = A_{jet} \cdot \left(1 - \frac{b}{a}\right) \cdot drop\_factor + \left(1 - drop\_factor \cdot \left(1 - \frac{b}{a}\right)\right) \cdot A_n \qquad (2.5)$$

For a straight inlet/outlet with no change in elevation the formula gives that the effective flow area equals the jet area.

If the jet area is affected by the bottom level of the manhole the jet area is reduced correspondingly.

If the effective flow area is greater than the full cross-section area of the manhole, A_m, then the full cross-section area will be used.

The manhole volume contributes to the overall system volume and is included in the computations.

If the water level exceeds the ground elevation H_{top}, then surface flooding occurs, consequently followed by appropriate treatment by the model (see section 8.1 Surface Flooding *(p. 101)*)

Structures (basins)

This type of nodes is associated with arbitrarily shaped structures of significant volume - non-circular manholes, tanks, reservoirs, basins and natural ponds.

Structure geometry is defined by a table of data sets (min two) related to monotonously increasing elevations, containing the following:

H =elevation, [m]

A_c =cross section area (used in calculation of the flow velocity in the structure, assuming uniform velocity distribution), [m²]

A_s =water surface area (used for calculation of volume), [m²]

K =outlet shape, types 1-9

The first set of values corresponds to the structure bottom. The last set corresponds to the surface level. Intermediate values are linearly interpolated. The H-column can start at any value, e.g. 0.0 for interpretation of H as depth in the basin. The MOUSE Engine will associate the first H-value to the bottom level of the node.

Definition of the outlet shape is connected with calculation of head losses in nodes (see section 7.2 Head Losses in Manholes and Structures - Introduction *(p. 88)*).

A structure volume contributes to the overall system volume and is included in the computations.

If the water level raises above the highest elevation value in the table describing the structure geometry, the program extends the basin geometry, following the principle as described in section 8.1 Surface Flooding *(p. 101)*.

An example of a definition of a basin is given in Figure 2.6.
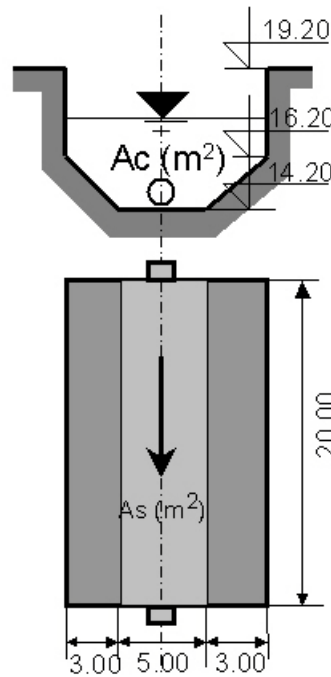
Figure 2.6   Definition of a basin – an example

Storage Nodes

Purpose of storage nodes is a controlled simulation of the surface flooding, i.e. controlled return of the water into the sewer system.

Storage nodes are fully defined with the identification string alone. The only other parameter associated with a storage node is the content of water (the capacity is not limited) currently stored in the storage node. Water enters a storage node from any manhole or structure, either through a weir, gate/orifice or a pump. A storage node may be emptied by an emptying function.

Outlets

Outlets are nodes specified at locations where the modelled system interacts with receiving waters. External water volume is assumed so large that the outlet water level is not affected by the outflow from the sewer system. As such, outlets are appropriate for simulation of the sewer flow recipients (river, lake, and sea).

An outlet can behave as an inlet, which depends on the flow conditions in the link, attached to the outlet and the water level specified at the outlet. This means that the flow in both directions can occur.

Outlets are defined with the following parameters:

H_{bott} = outlet bottom elevation, [m]
H_{out} = water surface elevation at outlet, [m]

Water surface elevation H_{out} can be specified as constant or as time dependent (see section 6 Boundary Conditions *(p. 79)*).

Depending on the specified outlet water level, the model applies the following elevation of the water surface H in the link adjacent to the outlet:

$$h = \begin{cases} H_{out} & for & H_{out} \geq H_{bott} + min(y_c \cdot y_n) \\ & else & \\ & H_{bott} + min(y_c \cdot y_n) & \end{cases} \qquad (2.6)$$

where:

y_c = critical depth, [m]
y_n = normal depth, [m]

In the later case, the outlet is considered to be a free outlet, meaning that the outlet water level does not influence the flow in the adjacent link.

Otherwise, the model applies the specified water level, with the corresponding backwater effect and a possibility for reverse flow.

2.4 Functions

Functions are used for the calculation of the flow between two nodes or in specified links according to the functional relation and the hydraulic conditions at relevant points in the system.

There can be more functions defined simultaneously between two nodes of the network. One or more functions can be defined in a link between the two nodes.

2.4.1 Overflow weirs

The overflow structures are normally found in sewer systems with purpose to lessen the hydraulic load in the pipe system during extreme flow conditions by allowing a part of the flow to be spilled to a recipient. Also, overflow structures can be used for internal distribution of the flow within the pipe system.

According to hydraulic conditions, two different types of overflow are possible:

- free overflow
- submerged overflow

The free overflow is the more frequent of the two types and the present conceptualisation is therefore concentrated on this phenomenon. The computation of the submerged overflow is based on the same concept as the free overflow and therefore inherently yields approximate results.

The following description covers weirs where it is acceptable to assume a constant water depth at the weir crest.

MOUSE also supports a weir where this assumption is not acceptable. This type of weir is called a "long" weir, please refer to the section concerning this type of element.

Definition of an Overflow Weir – General

Overflow weirs (structures) can be specified in nodes defined either as manholes or as structures, but not at an outlet. A weir is topologically fully defined with two node identifiers, defining the upstream node ('FROM') and downstream node ('TO').

The definition of the upstream and downstream nodes does not restrict direction of the flow because the weir function allows the flow in both directions, depending on the current hydraulic conditions. Practically, this means that if the water level in the downstream node is higher than the water level in the upstream node, then the water flows 'backwards', i.e. the computed flow rates are given a negative sign.

If an overflow structure discharges out of the contemplated pipe system then the downstream node identifier is left unspecified (empty).

The relation between the water level in the structure or manhole and the released discharge can be defined as a specific *Q/H* relation, or the built-in overflow formula can be used. In the later case, the discharge is calculated on the basis of a given structure geometry (crest elevation, structure width, orientation relative to the flow, crest type). It is important that the width of the overflow is realistic compared to the physical dimensions of the manhole or structure. E.g., an overflow width of 10 m in a manhole having a diameter of 2 m will inevitably cause numerical problems when the overflow is in function.

Q/H Relation

The user-defined *Q/H* relation consists of at least 2 pairs of tabulated values for water level above the weir crest, *H* [m], and corresponding discharge, *Q* [m^3/s]. Intermediate values are linearly interpolated.

The *Q/H* table has to fulfil certain conditions:

- the first *H*-value has to be the overflow (weir crest) elevation;
- the *H*-values have to be given in a monotonously increasing order;
- the largest *H*-value given in the table shall not be less than the largest *H*-value to be computed. The model does not extrapolate beyond the tabulated values.

Built in Overflow Formula

MOUSE provides two different methods for the computation of the free overflow:

- Flow computation based on the energy loss coefficient and weir orientation. **This is applied if the field for the discharge coefficient on the weir dialog is left empty.**
- Flow computation based on a standard rectangular overflow weir formula with user-specified discharge coefficient. **This is applied if a discharge coefficient is specified**.

Energy Loss Coefficient

In case of a free overflow, the water depth above the weir crest will be equal to the critical water depth. Certain energy loss occurs, with a magnitude depending on the structural configuration. The overflow situation is schematised in Figure 2.7.
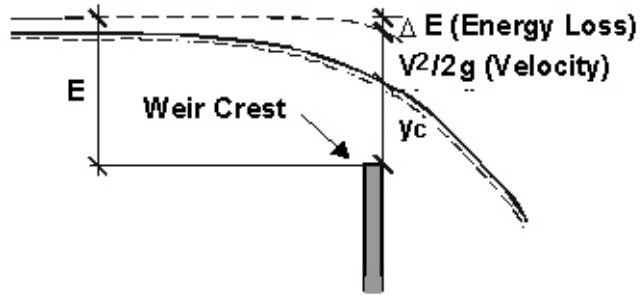
Figure 2.7   Free Overflow

In the critical flow section the Froude's number *Fr* equals to 1, and the critical flow condition can be written as:

$$Fr = \frac{v}{\sqrt{gy_c}} = 1$$

(2.7)

where:

v   =   mean flow velocity, [ms^{-1}]

y_c =   critical depth, [m]

g   =   9.81 [ms^{-2}]

Conservation of energy between the upstream and critical cross section yields with:

$$E = y_c + \frac{v^2}{2g} + \Delta E$$

(2.8)

with:

$$\Delta E = K_c \cdot \frac{v^2}{2g}$$

(2.9)

where:

E=   energy level at the section just upstream the structure, [m]
ΔE=entrance energy loss, [m]
K_c=   energy loss coefficient

Based on the energy conservation and critical flow principles, discharge over a plane overflow having a structure width B [m], is calculated for a weir orthogonal to the flow axis (90°), as:

$$Q_{weir} = B \cdot \sqrt{g} \cdot \left(\frac{2}{2 + K_c} \cdot H \right)^{\frac{3}{2}} \qquad (2.10)$$

and for a 'side' overflow weir (0°):

$$Q_{weir} = B \cdot \sqrt{g} \cdot \left(\frac{2}{3 + K_c} \cdot H \right)^{\frac{3}{2}} \qquad (2.11)$$

where:

H =   water depth above the weir crest level, [m]

K_c =   energy loss coefficient associated with the outlet head-loss, specified for the weir node (see sections
7.2 Head Losses in Manholes and Structures - Introduction *(p. 88)*
to 7.5 Selecting an Appropriate Local Head-loss Computation *(p. 93))*.

This actually corresponds to the standard overflow formula for a rectangular notch:

$$Q_{weir} = \frac{2}{3} \cdot C_d \cdot B \cdot \sqrt{2g} \cdot (H)^{3/2} \qquad (2.12)$$

where C_d is a discharge coefficient, expressed for an orthogonal weir as:

$$C_d = \frac{3}{(2 + K_c)^{3/2}} \qquad (2.13)$$

and for a 'side' overflow weir:

$$C_d = \frac{3}{(3 + K_c)^{3/2}} \qquad (2.14)$$

Where K_c is the head loss coefficient applied for the upstream manhole. E.g., this method if used with K_c = 0.5 (sharp-edged outlet), is equivalent to a standard weir formula with C_d = 0.7589 and C_d = 0.4582 for orthogonal and for side weir, respectively. Please note that the crest type - sharp or broad crested has no influence on the calculations.

The side overflow yields a smaller discharge for the same overflow level, because in this case the kinetic energy of the approaching flow is excluded from the computations.

User-Specified Discharge Coefficient

If the method with default energy loss coefficient is not applicable for a particular weir, the standard overflow formula Equation (2.12) is applied with a user-specified "level" discharge coefficient $C_H = 2/3C_d$, which gives:

$$Q_{weir} = C_H \cdot B \cdot \sqrt{2g} \cdot (H)^{\frac{3}{2}} \qquad (2.15)$$

This implies that the head-loss coefficient specified for the weir node and the weir orientation are ignored in the weir computation.

Submerged Overflow

The model calculates the flow rate for the submerged overflow using the same critical depth formulation in the case of a submerged overflow. In this situation, the head that is driving the flow is expressed as the difference between the upstream and downstream water surface elevations.
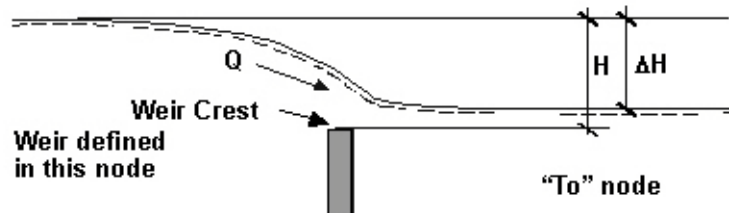
Figure 2.8   Principle of submerged overflow.

The submerged weir flow is then (with user-specified "level" discharge coefficient) approximated as:

$$Q_{weir} = C_H \cdot B \cdot \sqrt{2g} \cdot \frac{H}{\Delta H}(\Delta H)^{\frac{3}{2}} \qquad (2.16)$$

or with energy loss coefficient, for orthogonal overflow weir:

$$Q_{weir} = B \cdot \sqrt{g} \cdot \left(\frac{2}{2 + K_c} \cdot \Delta H\right)^{\frac{3}{2}} \cdot \frac{H}{\Delta H} \qquad (2.17)$$

and for a 'side' overflow weir (0º):

$$Q_{weir} = B \cdot \sqrt{g} \cdot \left(\frac{2}{3 + K_c} \cdot \Delta H \right)^{\frac{3}{2}} \cdot \frac{H}{\Delta H}$$

(2.18)

2.4.2   Orifice Function

Orifice is an opening of any shape, allowing water passage between otherwise separated parts of the network. Usually, an orifice represents a flow restriction.

Like an overflow weir, orifice is defined in MOUSE as a function between two nodes.

MOUSE supports the computation of flows through orifices of any shape, in all possible flow regimes. Further, a rectangular orifice with moveable top is used for the simulation of controllable rectangular sluice gates.

Orifice functions can be specified in nodes defined either as manholes or as structures, but not at an outlet. An orifice is topologically fully defined with two node identifiers, defining the orifice upstream node ('FROM') and the orifice downstream node ('TO').

Basic Geometrical Assumptions

Bottom is considered horizontal, both in the sections upstream and downstream from the orifice.

The upstream overflow crest height w_1 is calculated as the distance between the orifice invert level and the bottom level of the upstream node. Similarly, the overflow crest height from downstream, w_2 is given as the distance between the orifice sill level and the bottom level of the downstream node.

Other parameters are described in the following text or illustrated on drawings.

Approximation of Arbitrary Geometrical Shapes

An orifice opening is defined as a closed polygon through the MOUSE cross-section editor. Any form of convex and concave shapes is allowed, as long as there are no intersected arcs (see Figure 2.9).
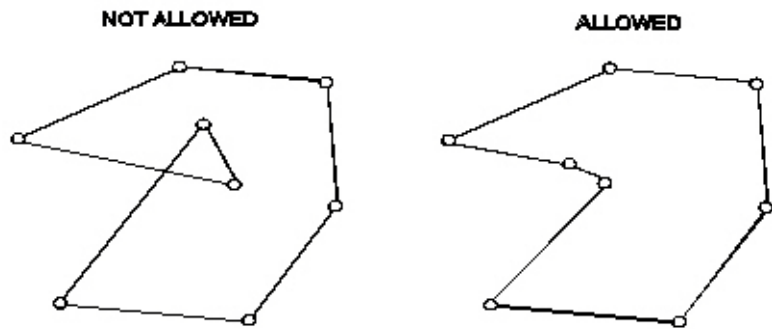
Figure 2.9   Examples of an "illegal" (left) and correct definition of an orifice polygon.

For the computational purpose, a polygon is cut into a number of narrow rectangles ('slices') which approximate the shape of an orifice (see Figure 2.10).
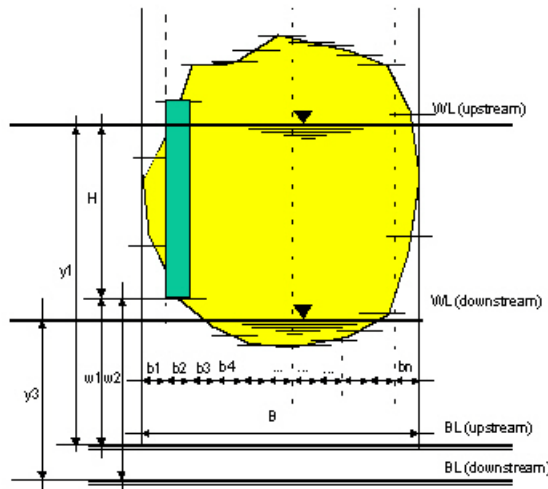
Figure 2.10   Illustration of a general shape orifice.

For the given upstream and downstream water levels, flow through the orifice is computed as an integral of the flows through individual slices, with the total flow corrected for lateral contraction.

Orifice Flow Regimes

Basically, there are four different types of flow regimes through an orifice (i.e. for individual slice) for the approaching flow in sub-critical regime. These are classified as:

- Free overflow,
- Submerged overflow,

- Free underflow, and
- Submerged underflow.

A definition sketch of the four types of flow regimes is shown on Figure 2.11.

Further, the theory distinguishes different forms of overflow jets, depending on the geometrical and hydraulic relations. In the current implementation, equations for the *ventilated jet* for the free overflow and the momentum equation for the *filled jet* (with a simplified correction for the downstream pressure) for the submerged case have been adopted. These types are the most common.

The solution for the approaching flow in super-critical regime has not been implemented.
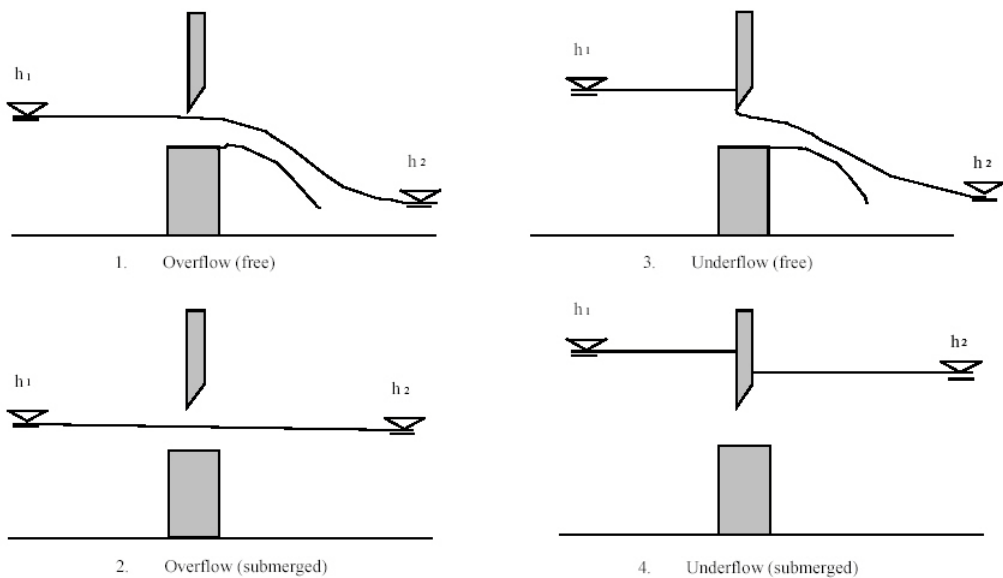
Figure 2.11   Flow regimes through an orifice.

Free Overflow

This flow regime is identified when the downstream water level has no influence on the discharge over the weir. The water surface is free, and the solution is therefore a pure free-overflow weir solution.

The weir is considered to be ventilated and sharp-crested. The discharge over a unit width of a weir for a given water level is given by:

$$q = C_H \cdot H \sqrt{2gH} \qquad (2.19)$$

q =   the discharge pr. m of the weir (m²/s).

H =   upstream water level above the crest (m).

C_H =   the "level" discharge coefficient for the sharp-crested weir, obtained as $C_H = 2/3 C_d$ (see section 2.4.1 Overflow weirs *(p. 25))*.

The coefficient C_H is given in Table 2.2 for different values of the weir height divided by the water level above the crest (w_1/H).

Table 2.2   *Variation of C_H for different values of w_1/H*

C_H	Value of w_1/H
$0.407 + \dfrac{0{,}0533}{w_1/H}$	> 0.2
0.673	0.2
0.757	0.1
0.761	0.05
$0.707\left(1 + \dfrac{w_1}{H}\right)^{1{,}5}$	<0.05

In the interval from w_1/H = 0.05 to 0.1 the coefficient C_H is interpolated linearly between 0.761 and 0.757. In the interval from $w1/H$ = 0.1 to 0.2 the coefficient is interpolated linearly between 0.757 and 0.673.

Ignoring the energy loss from the upstream section to the weir section, the energy equation reads:

$$E = H + \frac{\alpha q^2}{2g(H + w_1)^2} = y + \frac{\alpha q^2}{2g(\psi_v y)^2} \tag{2.20}$$

where:

y =   the distance from the sill level to the surface at the weir crest (m),

α =   the Coriolis factor;

ψ_v =   the vertical contraction coefficient;

E =   the energy level (m).

The depth at the weir crest is considered to be critical, i.e. $y = y_C = 2/3E$. This assumption is very rough, because the streamlines are curved. As a consequence, the depth over the crest will be less than the critical depth. In the context of the present implementation, curvature of the streamlines is ignored, since the expression is only used to evaluate the effect the velocity

term have on the coefficient C_H. The effect of curved streamlines is indeed incorporated in the coefficients C_H and C_E.

By inserting $y = 2/3E$ on the right hand side of Equation (2.20), the following relation is obtained:

$$E = \frac{2}{3}E + \frac{\alpha q^2}{2g\psi_v^2\left(\frac{2}{3}E\right)^2} \Rightarrow q = \psi_v\sqrt{\frac{4}{27\alpha}}E\sqrt{2gE} = C_E E\sqrt{2gE} \qquad (2.21)$$

where:

C_E the energy discharge coefficient for the sharp-crested weir.

Since the discharge q can be expressed either via the water level above the crest upstream of the weir, or the energy level at the upstream section, the following relation between the level discharge coefficient and the energy discharge coefficient can be derived:

$$C_H = C_E\left[1 + \frac{\alpha q^2}{2gH(w_1 + H)^2}\right]^{\frac{3}{2}} \qquad (2.22)$$

As it can be seen from the relation above, the coefficient C_H takes several effects into account. One effect is the change of the velocity term in the energy equation ($v^2/2g$). For large values of w_1 is the upstream energy level E approximately equal to the depth over the crest H and C_E is equal C_H. For smaller values of w_1, the upstream velocity term becomes more important and C_E and C_H will deviate from each other. The other effects are the curved streamlines, the change in the Coriolis coefficient (α), the vertical contraction coefficient (ψ_v), the surface tension and the friction. The latter effects influence both C_E and C_H.

By moving from a (q,H) relation to a (q,E) relation, the variation in the discharge coefficient should be expected to be smaller.

The energy level is given as:

$$E = H + \frac{\alpha v^2}{2g} = H + \frac{\alpha q^2}{2g(H + w_1)^2} = \beta_1 H \qquad (2.23)$$

where:

β_1 Coefficient of the relation between energy and water level.

By combining Equations (2.23) with (2.22), β_1 can be expressed as:

$$\beta_1 = 1 + C_H^{\ 2} \left\{ \frac{1}{1 + \left(\dfrac{w_1}{H}\right)} \right\}^2 \tag{2.24}$$

and the coefficient C_E can be expressed as:

$$C_E = \frac{C_H}{\beta_1^{3/2}} \tag{2.25}$$

The table below shows the relation between C_H, C_E, β_1 and q (for $H = 1$) for different values of w_1/H, showing indeed that the coefficient C_E shows less variation than the values for C_H.

Table 2.3   *Relations between CH, CE, β, q, E for different values of w_1/H*

w_1/H	C_H	C_E	β	Q for H=1	E	$1.71E^{3/2}$
∞	0.407	0.407	1.00	1.81	1.000	1.71
1	0.460	0.426	1.053	2.04	1.053	1.84
0.1	0.757	0.423	1.474	3.35	1.474	3.05
0.05	0.761	0.404	1.525	3.37	1.525	3.22
0	0.707	0.385	1.500	3.13	1.500	3.15

Starting with values for H and w_1 given, the energy level can be derived by iteration. The iteration implemented in the program is based on a Newton-Raphson technique.

The discharge over the weir can then be determined by inserting the energy level into equation (2.21).

Submerged Overflow

The submerged overflow is identified when the downstream water level influences the discharge over the weir, and water surface is free (i.e. the upper of the gate is not in contact with the water surface, as can be seen in Figure 2.11). The submerged overflow case will be applied, when the $w_0/H \geq$ 1.0 and $\Delta H/H \leq 1/3$, where wo is the height of the orifice and H is the water depth above the sill level.

The submerged overflow case is illustrated in Figure 2.12, also giving the meaning of the geometrical parameters used in the sequel.
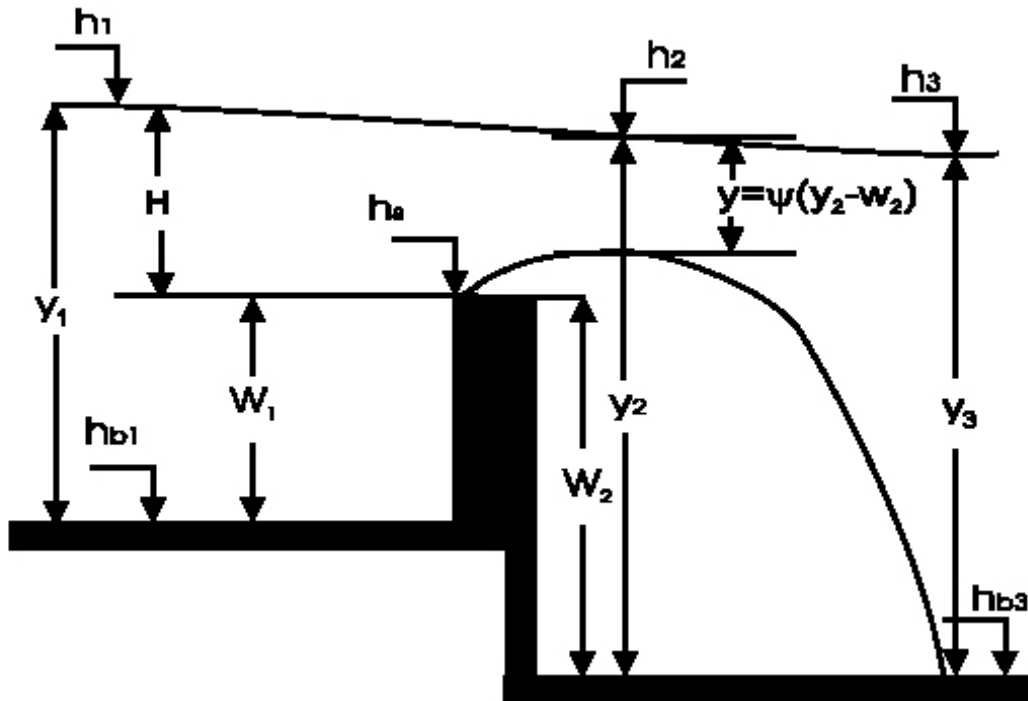
Figure 2.12 Definition fo submerged overflow

Since the energy loss from section 1 to 2 is much smaller than the energy loss from 2 to 3, the energy loss is neglected (i.e. $E_1 = E_2$). The energy equation now reads:

$$y_1 - w_1 + \frac{q^2}{y_1^2 2g} = y_2 - w_2 + \frac{q^2}{y^2 2g} \tag{2.26}$$

The momentum equation from section 2 to 3 can be written as:

$$\frac{q^2}{gy} + \frac{y_2^2}{2} = \frac{q^2}{gy_3} + \frac{y_3^2}{2} \tag{2.27}$$

where the shear stress on the bottom between section 2 and 3 is neglected. The contracted overflow area can be expressed by applying the vertical contraction coefficient given as $y = \psi_v \,(y_2\text{-}w_2)$.

There are two unknowns in these two equations. By rearranging the equations and substituting the q (actually $q^2/2g$) from one of the equations into another, the remaining unknown in the obtained equation is y_2.

The equation can be transformed into a 4th degree polynomial, of a general form:

$$C_4 y_2{}^4 + C_3 y_2{}^3 + C_2 y_2{}^2 + C_1 y_2 + C_0 = 0 \qquad (2.28)$$

The polynomial is solved iteratively, applying the Newton-Raphson principle. The initial value of y_2 applied in the iterations is $y_2 = y_1 - w_1 + w_2 - (1/2)\Delta H$.

The iterative process terminates when y_2 converges within the specified threshold, or if the number of iterations exceeds the specified number. If the convergence is achieved, the discharge can then be derived from equation (2.26).

The value of y_2 is rejected, if the maximum number of iterations is exceeded or in the following cases:

- If y_2 gives a negative argument to the square-root for the discharge,
- If $y_2 > y_1 - w_1 + w_2$ or $y_2 < w_2$.

The equations applied above have some shortcomings. At first, the effect of the curved streamlines is not taken into account properly, in contrast to the free overflow case (which is derived from empirical expressions). The curved streamlines will in this case give a different pressure distribution over the crest deviating from the hydrostatic pressure and the pressure will be smaller. The curved streamlines will become less and less important, the smaller the values of $\Delta H/H$ are. Secondly, the contraction coefficient has a significant effect on the discharge, e.g. this approach is very sensitive to the choice of the vertical contraction coefficient.

The submerged overflow solution must be compatible with the free overflow at the transition between the two flow regimes. In other words, introducing the submerged solution at $\Delta H/H = 1/3$ requires that the submerged discharge for this water level difference is equal to the free flow discharge. This is not achievable in all cases and sometimes another pragmatic solution must be adopted for the transitional regime.

Following the approximate rule as for the flow over a broad-crested weir, a flow reduction is introduced as soon as the difference between upstream and downstream water level is less than one third of the upstream water level. The remaining submerged discharge is proportional to the square root of the difference in upstream and downstream water levels above the weir crest. The free flow is taken from the "sharp-crested" case, as described above.

The flow in the submerged flow can be approximated as:

$$q = \frac{q_f}{\sqrt{\frac{1}{3}}} \sqrt{\frac{\Delta H}{H}}; for \frac{\Delta H}{H} \le \frac{1}{3} \qquad (2.29)$$

where:

ΔH the water level difference between the upstream and down-
stream section,

q_f the free flow at the level where ΔH= 1/3.

The implemented algorithm includes a combination of the parabolic and the momentum solution. The parabolic solution is applied, if the combined energy and momentum equation does not give applicable solutions for the given ΔH/H (i.e. if y_2 is rejected). The discharge is solved for decreasing values of ΔH/H and for each value *of ΔH/H < 1/3* is the combined energy and momentum equation evaluated. As soon as the combined energy and momentum equation begin to give applicable solutions, a swap from the approximate parabolic solution to the combined energy and momentum solution is performed. The contraction coefficient will in this case be based on the criteria, that the discharge applying the combined momentum and energy solution is the same as from the parabolic solution, at the point of intersection.

Free Underflow

The underflow is free, if the issuing jet of the supercritical flow is open to the atmosphere and is not overlaid or submerged by tail water. Following an approach similar to the one developed in the section related to free overflow, the discharge through the opening (e.g. gate) can be expressed as:

$$q = C_E w_o \sqrt{2gE_1}$$ *(2.30)*

where:

q	the specific discharge,
E_1	the energy level upstream of the opening,
w_o	the gate opening,
C_E	the discharge coefficient with respect to the energy level.

The energy level at the upstream side can be expressed as:

$$E = H + \frac{q^2}{2g(H + w_1)^2} = \beta_2 H$$ (2.31)

where:

H	the upstream water level measured from the crest of the weir,
q	the discharge,
w_1	is the weir height at the upstream side.

Usually, discharge is given as a function of the upstream water depth above the crest, rather than by energy level:

$$q = C_H w_o \sqrt{2gH} \tag{2.32}$$

with:

$$C_H = \frac{C_c}{\sqrt{1 + C_c \dfrac{w_o}{H + w_1}}} = \frac{C_c}{\sqrt{1 + C_c \dfrac{\dfrac{w_0}{H}}{1 + \dfrac{w_1}{H}}}} \tag{2.33}$$

where C_c is a constant representing the contraction coefficient of the jet.

Substitution of equation (2.33) into equation (2.32) leads to the expression:

$$\beta_2 = 1 + C_H{}^2 \left(\frac{\dfrac{w_o}{H}}{1 + \dfrac{w_1}{H}} \right)^2 \tag{2.34}$$

Further, the relationship between C_E and C_H may be derived as:

$$C_E = \frac{C_H}{\sqrt{\beta_2}} \tag{2.35}$$

From above equations, the underflow discharge can be computed. However, it should be noted that the compatibility of discharge values at the transition from the free overflow equation to the free underflow equation must be secured. Theoretically, this transition should take place at the moment where the upstream water level touches the top of the gate. This point is difficult to define as the water level is drawn down towards the contracted section. Another complication is the fact that the underflow equation is accurate only for upstream depths considerably exceeding the depth of the gate opening.

For this reason, the transition is simply assumed to take place at an upstream water level equal to the top of the gate, while the difference between overflow and underflow equations is fully corrected in the underflow computation at that level. This requires a correction in the free underflow equation, through the use of a correction coefficient.

For increasing upstream water levels, this correction coefficient is gradually reduced as follows:

$$C_{new} = C_c - \delta(C_c - C_E)$$

(2.36)

where:

$$\delta = \left(C_c - \frac{q_{overflow}}{(w_0\sqrt{(2gE)})} \right)(C_c - C_E)$$

(2.37)

with E and C_E taken at the top of the gate level. For increasing upstream levels the discharge coefficient approaches the constant value C_c, usually taken as 0.608.

The free flow equations require a further correction based on the pressure distribution at the outflow side.

There are two extreme cases, the jet can either emanate surrounded by free atmosphere (like an orifice), or it can have full contact with the bottom on the downstream side (the vertical sluice gate).

In the first case the pressure over the height of the jet is approximately atmospheric. In the other case the pressure follows a hydrostatic distribution. The real situation usually is somewhere in between these two extreme cases, and the flow through the gate is corrected for the influence from the pressure on the downstream side.

The underflow equation has been derived on the basis of experiments where the downstream bottom level is the same as the sill level of gates ($w_2 = 0$). This implies a hydrostatic pressure distribution in the contracted flow section. With positive values for w_2 (drop structure), however, these pressures drop to lower values, with nearly atmospheric pressure over the height of the jet. In this case the discharge will be higher due to the lower counter pressure. Comparison of the orifice flow equation and the underflow equation reveals that this difference may be up to 9 %. The same reasoning applies, to some extent, for the case of overflow, where the discharge equation for the case of a free overfall ($w_1 = 0$) is also based on hydrostatic pressure distribution assumption.

To cover most cases in a reasonable way, therefore, the free flow discharges are increased by 5 % for the case where the downstream water level is found below the crest level of the gate. For the range of downstream water levels between the crest level and the upstream level, the correction applied is reduced quadratically as the downstream water level is increasing. The quadratic reduction follows from the quadratic relation between the integrated hydrostatic pressure force and the water depth. Although the matrix of free flow discharges is set up for the complete range of downstream water levels

up to the level which equals the upstream level, it should be realised, that some of these corrected discharges are overwritten by new values for the submerged flow case.

Submerged Underflow

The submerged underflow is identified when the upstream water level is above the gate level and the downstream water level influences the discharge through the gate. The threshold for swapping from free underflow to submerged underflow is, for the simplification purpose, defined at $\Delta H/H = 1/3$. This ensures that the same criterion is applied both in the overflow and underflow cases and a consistency of the solution is maintained when w_0/H approaches unity.

A definition sketch of the submerged underflow is shown in Figure 2.13.
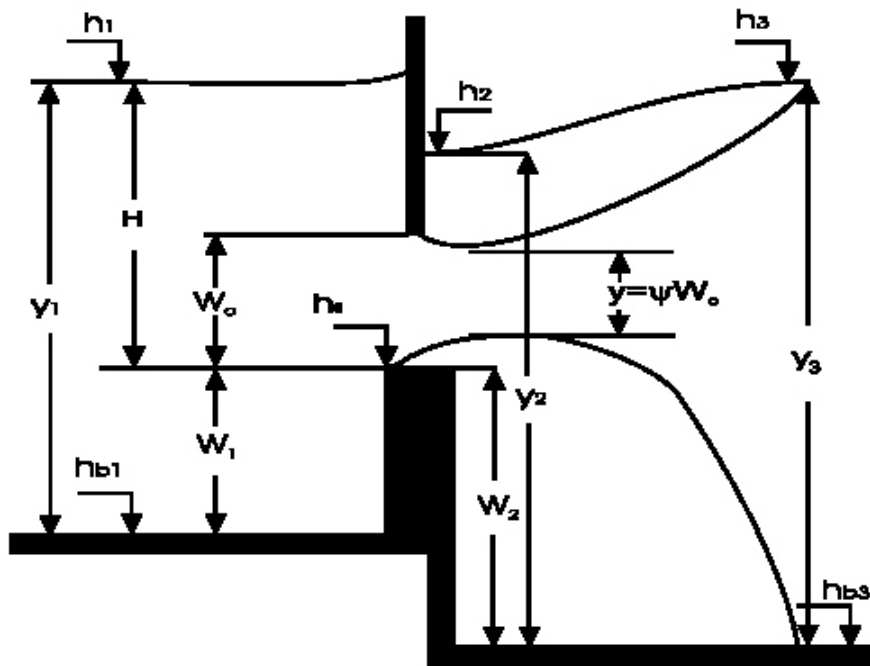
Figure 2.13 Definition of submerged underflow.

A combined energy and momentum formulation is applied (the same principle as for the submerged overflow). If the energy loss from section 1 to 2 is ignored, the energy equation reads:

$$y_1 - w_1 + \frac{q^2}{y_1^2 2g} = y_2 - w_2 + \frac{q^2}{y^2 2g}$$ (2.38)

The momentum equation from section 2 to 3 can be written as:

$$\frac{q^2}{gy} + \frac{y_2{}^2}{2} = \frac{q^2}{gy_3} + \frac{y_3{}^2}{2}$$

(2.39)

where the shear stress on the bottom from section 2 and 3 is neglected. The contracted overflow area can then be expressed by applying the vertical contraction coefficient given as $y = \psi_v w_0$.

By rearranging the two equations and eliminating one of the two unknowns (q and y_2), the combined equation reads:

$$(y_2 - w_2 - y_1 + w_1) - \frac{1}{4}(y_3^2 - y_2^2)\left(\frac{1}{y_1^2} - \frac{1}{(\psi_v w_0)^2}\right) = 0$$

(2.40)

Introducing the constants $C_1 = (1/(\Psi_v w_0) - 1/y_3)$ and $C_2 = (1/y_1{}^2 - 1/(\Psi_v w_0)^2)$, the equation can be reduced to a second degree polynomial in the form:

$$\frac{1}{4}C_2 y_2^2 + C_1 y_2 + \left(C_1(w_1 - w_2 - y_1) - \frac{1}{4}C_2 y_3^2\right) = 0$$

(2.41)

Introducing:

$$A = (1/4)C_2, \quad B = C_1, \quad C = C_1(w_1 - w_2 - y_1) - (1/4)C_2 y_3{}^2$$

(2.42)

it can be shown that the only realistic solution for the second-degree polynomial, is the negative one. So, y_2 can be expressed as:

$$y_2 = \frac{-B - \sqrt{B^2 - 4AC}}{2A}$$

(2.43)

and the discharge can then be derived from equation (2.38).

The solution is sensible to the selection of the vertical contraction coefficient. The contraction coefficient must be determined, so that smooth transition between free and submerged underflow is maintained.

For a certain range of contraction coefficient values, only imaginary solutions to the Equation (2.43) exist. In such cases, i.e. as long as the combined energy and momentum equation fail to deliver reasonable results, the parabolic solution is applied, similarly as for the transition between free and submerged overflow.

Practical Computational Aspects

Computation of the flows through an orifice is based on a pre-processed 4-D table, containing the flows through a vertical slice of unit width, computed as a function of four dimensionless parameters: w_0/H, w_1/H, w_2/H and $\Delta H/H$, and using the equations described in previous paragraphs. The 'unit' flows are computed at discrete points determined by the following set of the dimensionless parameter values:

w_0/H = {0.00, 0.05, 0.10, 0.30, 0.50, 0.80, 1.00}
w_1/H = {0.00, 0.05, 0.10, 0.30, 1.00, 5.00, 100.00}
w_2/H = {0.00, 0.05, 0.10, 0.30, 1.00, 5.00, 100.00}
$\Delta H/H$ ={0.00, 0.01, 0.04, 0.09, 0.16, 0.25, 0.36, 0.49, 0.64, 0.70, 0.80,
　　　　　　0.85, 0.90, 0.95, 1.00}

This table is stored in a binary file *MOUSE650.ORI* and is supplied as a part of MOUSE installation.

At the simulation start, MOUSE generates a structure-specific 3-D table for each orifice, where actual flows to be applied in the computation are stored. This table, of the size 28 x 28 x 10 contains discharges for all the combinations of 28 upstream and downstream water levels, covering the full range of possible water levels. When the algorithm is used for a gate, the third dimension is used for 10 different gate openings.

A non-equidistant scaling (approximating logarithmic scaling) is applied for the water levels, while the scaling of the gate position is linear.

During the pre-processing, the following operations are executed:

- Grids for the full range of upstream and downstream water levels are generated. The grid spacing depends on the local geometrical parameters.

- Discharge from the dimensionless 4D-table, for the given upstream and downstream water level and, if relevant gate position, are read and interpolated.

- The 'unit' discharges are scaled, by multiplying the discharge by the upstream depth above the crest (i.e. slice bottom) to the power of 1.5 ($H^{1.5}$).

- The discharge is corrected (reduced) for the effect of lateral contraction.

- The discharge for entire orifice is summed up.

The actual flow through an orifice in a given hydraulic situation is obtained during the simulation, by interpolating the flow derivatives with respect to h_1, h_2 and w_0 in the 3-D table, and inserting these directly into the MOUSE pipe flow algorithm. By these means, accuracy and stability of the computation is preserved, even with very rapid water level changes and fast movement of the gate.

2.4.3   Pump Function

Pump functions can be specified in nodes defined either as manholes or as structures, but not at an outlet. A pump is topologically fully defined with two node identifiers, defining the pump-sump basin node ('FROM') and the downstream (recipient) node ('TO').

If the pump discharges out system then the downstream node identifier ('TO') is left unspecified (empty).

The pump operation is specified by defining the range of operation: 'start level' H_{start}, [m], and 'stop level' H_{stop}, [m], and one of the two available relations in a form of tabulated pairs of values: (1) ΔH [m] and Q_{pump} [m³/s], or (2) H [m] and Q_{pump} [m³/s]. The Q_{pump}/H table consists of min two data sets, there is no upper limit. Intermediate values are linearly interpolated. Variables H, H_{start} and H_{stop} denote water level in a pump sump basin (pump wet well node).

Relation 1 correlates water level in the pump-sump basin and the pump discharge:

$$Q_{pump} = \begin{cases} Q(H) \text{ if } H_{stop} \leq H \\ \text{ or if } H_{start} \leq H \\ \quad else \\ \quad\quad 0 \end{cases}$$

(2.44)

Relation 2 defines the pump performance as a function of the water level difference between the two nodes:

$$Q_{pump} = \begin{cases} Q(\Delta H) \text{ if } H_{stop} \leq H \\ \text{ or if } H_{start} \leq H \\ \quad else \\ \quad\quad 0 \end{cases}$$

(2.45)

A number of pumps with different operation strategies can be simultaneously defined between the two nodes.

As the pump performance can be quite significant even during the start-up, it has been necessary to dampen the pump dynamics in order to sustain the numerical stability. The dampening is obtained by centring the pump rate backwards in time so that the pump performance does not instantaneously reach the full capacity but instead the pump discharge is gradually increased over some time steps.

If pumps are present in the model set-up it might be necessary to introduce relatively small time steps (5 - 10 sec.).

2.4.4 Flow Regulation

In computational terms the flow regulation differ fundamentally from the weir, orifice and pump function by the fact that the control is simulated within the pipe connecting two nodes and NOT by replacing the pipe with a functional relation. This means that the conduit connecting the two
specified nodes is treated by the algorithm as a normal link. The flow is controlled by setting the general equation coefficients at the control location (first upstream Q-point in the pipe).

The control function is specified as a function of water level in a control node A. The control is applied only within the specified range of water levels, and if the water level is outside the specified range, an unregulated flow applies. Therefore, it is important that the specified range covers all expected water levels at point A. Otherwise, a sharp transition between the Q defined by the control function, and 'natural' (unregulated) discharge would occur at the range bounds causing numerical instabilities.

The following expression determines the flow:

$$Q_{reg} = \begin{cases} min\{Q(H_A), Q_{nat}\} & for & H_{min} \leq H_A \leq H_{max} \\ & else \\ Q_{nat} \end{cases} \tag{2.46}$$

where:

Q_{reg}	=	applied (regulated) discharge, [m³s⁻¹]
$Q(H_A)$	=	discharge defined by the regulation function, [m³s⁻¹]
Q_{nat}	=	"natural" (unregulated) discharge, obtained as an explicit estimate, based on the known water levels in the previous time step on each side of the regulation point, [m³/s]
H_A	=	water level at the control point A, [m]
H_{min}, H_{max}	=	water levels at the control point A defining the range in which the regulation is to be applied, [m].

2.4.5 Non-return Valve

The function for simulation of non-return valves is included into the model structure identically as the flow regulation function.

The flow is applied according to the following:

$$Q_{reg} = \begin{cases} Q & for \quad H_{up} \geq H_{down} \\ & else \\ & 0 \end{cases}$$ (2.47)

where:

Q	=	calculated discharge, [m³s⁻¹]
Q_{reg}	=	applied discharge, [m³s⁻¹]
H_{up}, H_{down}	=	water levels at the computational points upstream and downstream, respectively, [m].

2.4.6   Combined Regulation (non-return valve + regulation)

A combination of the two previous functions results with:

$$Q_{reg} = \begin{cases} \min\{Q(H_a), Q_{nat}\} \; for \; H_{min} \leq H_A \leq H_{max} \; and \; (H_{up} \leq H_{down} \\ else \\ 0 \end{cases}$$ (2.48)

where:

Q_{reg}	=	applied discharge, [m³s⁻¹]
$Q(H_A)$	=	discharge defined by the regulation function, [m³s¹]
Q_{nat}	=	"natural" discharge, obtained as an explicate estimate, based on the known water levels in the previous time step on each side of the regulationpoint,[m³s¹]
H_A	=	water level at the control point A, [m]
H_{min}, H_{max}	=	water levels at the control point A defining the range in which the regulation is to be applied, [m]
H_{up}, H_{down}	=	water levels at the computational points upstream and downstream, respectively.

2.4.7   Long Weirs

A long weir is an element, which is able to simulate variations in the water depth above the weir crestalong the weir itself.

The long weir must be defined as a link between two channels of the "natural channel" type. The weir is topographically defined by the two links defining the upstream link ("Source channel") and the downstream link ("Destination channel"). The "Location" field is the upstream node of the source channel and the "To" field is the upstream node of the destination channel.

Discharge over the weir is calculated at each h-point in the upstream/downstream channel. Thus an internal weir, linking two branches require that the number of computational points in the two branches is the same.

The weirs must always link two open channels.

Description of the Flow - the Long Weir

For free flow conditions the weir discharge per length of weir will be calculated as:

$$q_s = \frac{2}{3} C_d \sqrt{2g} H^{3/2} \tag{2.49}$$

where

H	=	the water level above the weir crest,
C_d	=	the weir coefficient
g	=	the gravity constant

For submerged weir the flow conditions are defined as

$$q_s = \frac{2h}{3h_d} C_d \sqrt{2g} \Delta H^{3/2} \tag{2.50}$$

where

ΔH	=	the different between upstream and downstream water levels
h	=	the upstream depth over crest level
h_d	=	height of the weir.

The Saint Venant Equations are solved for conservation of mass and conservation of momentum. The equations are rewritten and solved for q and h points.

Conservation of mass (h-point):

$$\frac{\partial Q}{\partial x} + \frac{\partial A}{\partial t} = 0 \tag{2.51}$$

Conservation of momentum (q-points):

$$\frac{\partial Q}{\partial t} + \frac{\partial \left(\alpha \frac{Q^2}{A} \right)}{\partial x} + gA \frac{\partial y}{\partial x} + gAI_f = gAI_0 \tag{2.52}$$

where

Q	=	the flow
A	=	the flow cross section
y	=	the depth of water
I_f	=	the friction slope
I_0	=	the bottom slope of the canal

Taking into account the continuous discharge over the weir, Equation (2.52) is modified to

$$\frac{\partial Q}{\partial x} + \frac{\partial A}{\partial t} = q_s \tag{2.53}$$

In branches with long weirs the pair of equations (2.52) and (2.53) is solved.

The implementation of long weirs will include the possibility of specifying a variation of the weirs crest along the weir, for example a sloping weir crest. For this type of weirs, MIKE URBAN will divide the weir into a series of smaller sections (equal to the number of computational points) and apply an average crest level in each of these sections.

2.4.8 Valves

Implementation in MIKE URBAN

It is possible to define a valve between any internal nodes, but not at an outlet. The valve will be topologically fully defined with two node identifiers, defining the upstream node ('FROM') and downstream node ('TO').

The definition of the upstream and downstream nodes does not restrict the direction of the flow because the valve function allows the flow in both directions, depending on the current hydraulic conditions. Practically, this means that if the pressure level in the downstream node is higher than the pressure level in the upstream node, then the water flows 'backwards', i.e. the computed flow rates are given a negative sign. All valves can be defined either to be non return valves, meaning that only flow in the positive direction is allowed, or non restricted valves allowing flow in both directions.

The valve will apply the flow equation(2.54)

$$Q = A \sqrt{\frac{2g\Delta H}{k}} \tag{2.54}$$

where

g =   the gravity constant
k =   the flow factor which depends on the opening of the valve.
A =   full open flow area of the valve
ΔH =   the energy drop over the valve.

An assumption for this equation is that the valve is located in a pipe which is running under pressure. However, should the system run under non-pressurized flow conditions the flow area A in equation (2.54) of the valve is reduced by a linear reduction for non pressurized flow conditions:

$$A(d) = A\left(\frac{d}{d_f}\right) \qquad (2.55)$$

where

d   =   the depth of the flow depth
d_f =   the pressurized flow depth

This means that the velocity head upstream and downstream of the valve is equal and equation (1) can be rewritten to

$$Q = A\sqrt{\frac{2gh}{k}} \qquad (2.56)$$

where

h =   the drop in pressure over the valve.

MIKE URBAN supports full RTC control features of the new valve, which means that it will be possible to define control algorithm for the opening of valve.

3 Description of Unsteady Flow in Links

3.1 Saint Venant Equations – General

Computations of the unsteady flow in the links MOUSE Pipe Flow Model, applied with the dynamic wave description, performs by solving the vertically integrated equations of conservation of continuity and momentum (the 'Saint Venant' equations), based on the following assumptions:

- the water is incompressible and homogeneous, i.e. negligible variation in density;

- the bottom-slope is small, thus the cosine of the angle it makes with the horizontal may be taken as 1;

- the wavelengths are large compared to the water depth. This ensures that the flow everywhere can be regarded as having a direction parallel to the bottom, i.e. vertical acceleration can be neglected and a hydro-static pressure variation along the vertical can be assumed;

- the flow is sub-critical (Super-critical flow is also modelled in MOUSE, but using more restrictive conditions).

The general form of the equations takes the form as follows:

Conservation of Mass ('continuity equation')

$$\frac{\partial Q}{\partial x} + \frac{\partial A}{\partial t} = 0 \tag{3.1}$$

Conservation of Momentum ('momentum equation')

$$\frac{\partial Q}{\partial t} + \frac{\partial \left(\alpha \frac{Q^2}{A} \right)}{\partial x} + gA\frac{\partial y}{\partial x} + gAI_f = gAI_0 \tag{3.2}$$

where:

Q	=	discharge, [m^{3}s^{-1}]
A	=	flow area, [m^2]
y	=	flow depth, [m]
g	=	acceleration of gravity, [ms^{-2}]
x	=	distance in the flow direction, [m]
t	=	time, [s]
α	=	velocity distribution coefficient
I_0	=	bottom slope
I_f	=	friction slope

The derivation of these equations is described in a number of textbooks and scientific papers.

The general flow equations are non-linear, hyperbolic partial differential equations. The equations determine the flow condition (variation in water depth and flow rate) in a pipe or channel when they are solved with respect to proper initial and boundary conditions. Analytical solutions are only possible in special cases with a rather limited number of applications, therefore the general equations have to be solved numerically.

3.2   Implementation of the Saint Venant Equations in MOUSE

The Saint Venant equations can be rewritten as follows:

$$\frac{\partial Q}{\partial x} + \frac{\partial A}{\partial t} = 0 \tag{3.3}$$

and

$$\frac{\partial Q}{\partial t} + \frac{\partial \left(\alpha \frac{Q^2}{A}\right)}{\partial x} + gA\frac{\partial y}{\partial x} = gA(I_0 - I_f) \tag{3.4}$$

with the same nomenclature as for Equations (3.1) and (3.2). The sketch of the system being described by the equations is presented in Figure 3.1.
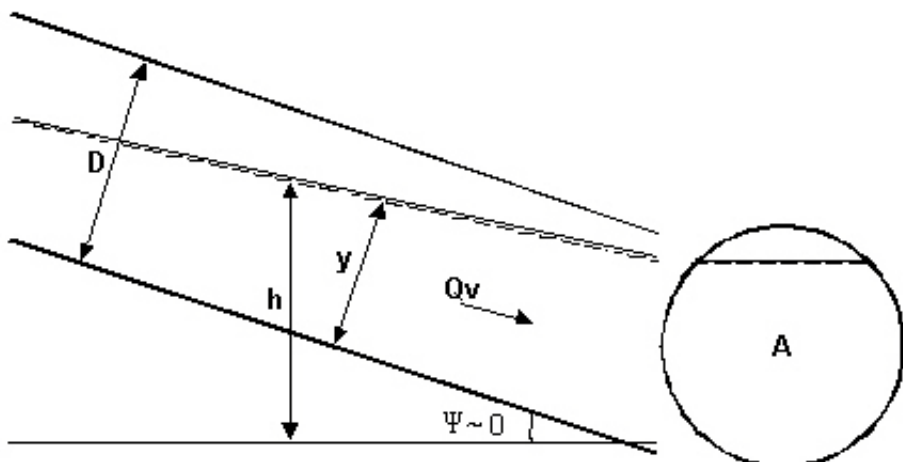

Figure 3.1   Sketch of the pipe section.

The equations above are valid for free surface flow only. They can, however, be generalised to include flow in full pipes (pressurised flow) as discussed in section 3.3 Modelling The Pressurised Flow *(p. 54)*.

The continuity equation expresses that the volume of water, ∂Q, which is added in pipe section of length ∂x, is balanced by an increase in cross-sectional area ∂A (storage).

The first two terms on the left side of the momentum equation represent the inertia forces (local and convective acceleration), while the third term represents pressure forces. The two terms on the right hand side of the equation represent gravity and friction forces, respectively.

The velocity distribution coefficient accounts for an uneven velocity distribution across a section and corresponding difference in the actual momentum, compared to those obtained with an average velocity. It is defined as:

$$\alpha = \frac{A}{Q^2}\int_A v^2 dA \tag{3.5}$$

Assuming that the bottom slope I_o is small ($\psi \sim 0$), then I_o can be expressed as a function of the water depth and water surface gradient, i.e.:

$$I_0 \approx \frac{\partial y}{\partial x} - \frac{\partial h}{\partial x} \tag{3.6}$$

It is thus possible to use the height, *h*, above a certain reference level, as the dependent variable instead of the water depth, *y*. The equation of momentum can hence be written as:

$$\frac{\partial Q}{\partial t} + \frac{\partial\left(\alpha\frac{Q^2}{A}\right)}{\partial x} + gA\frac{\partial h}{\partial x} = gAI_f \tag{3.7}$$

Pressure and gravity forces can be expressed in one term only as:

$$gA\frac{\partial h}{\partial x} \tag{3.8}$$

The friction slope I_f is equal to the slope of the energy grade line and is introduced into the equation using the Manning's formulation (for more details see section 4 Numerical Solution of the Flow Equations in MOUSE Link Networks *(p. 63)*).

3.3   Modelling The Pressurised Flow

The full flow capacity of a closed conduit (pipe) can be defined as a discharge at which the flow depth is equal to the conduit height. Any further increase of discharge fundamentally changes the conditions of flow, i.e. basic assumptions for the derivation of the Saint Venant equations are not valid. Namely, the flow changes from the free surface flow to the pressurised flow.

However, it is possible to generalise the equations for free surface flow, so that the pressurised flow in closed conduits is covered. This is done by introducing a fictitious slot in the top of the conduit, see Figure 3.2.

The idea of introducing a fictitious slot was first presented by Preissmann and Cunge, 1961, and has since been used by Cunge and Wegner, 1964 (see ref. /4/).

The derivation can be obtained from the continuity equation which can be written as:

$$-\frac{\partial(\rho Q)}{\partial x}dxdt = \frac{\partial(\rho A)}{\partial t}dxdt \tag{3.9}$$

assuming the density of water ρ constant over the cross section.
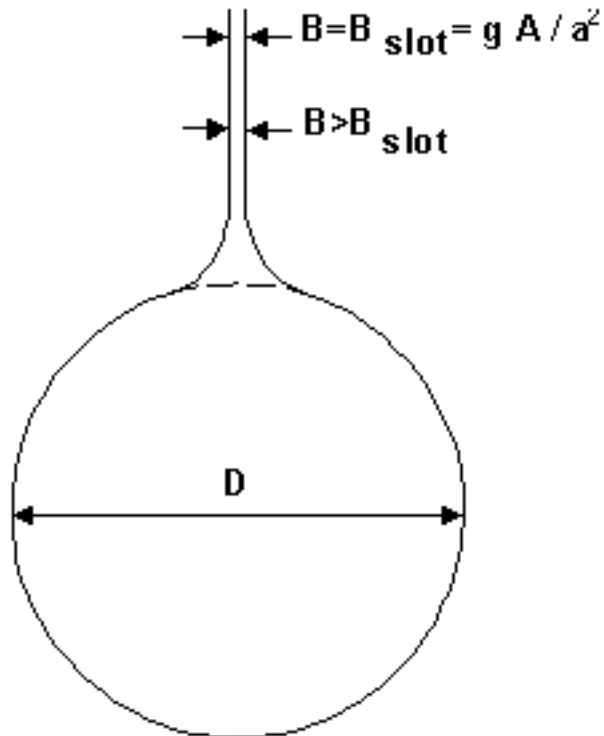
Figure 3.2   Pipe with a fictitious slot

By partial differentiation is found:

$$\frac{\partial Q}{\partial x} + \frac{Q}{\rho} \cdot \frac{\partial \rho}{\partial x} + \frac{\partial A}{\partial t} + \frac{A}{\rho} \cdot \frac{\partial \rho}{\partial t} = 0 \qquad (3.10)$$

For a circular pipe, it can be shown that the density of the water can be approximated as:

$$\rho \approx \rho_0 \left(1 + \frac{g(y-D)}{a_0^2} \right) \qquad (3.11)$$

where:

ρ_0	=	the density of water for a free surface flow [kgm^{-3}]
a_0	=	the speed of sound in water [ms^{-1}]
y	=	the water depth [m]
D	=	the pipe diameter [m].

Furthermore, it can be shown that the cross-sectional area in the case of the excess pressure $\rho g(y-D)$ approximately equals to:

$$A \approx A_0\left(1 + \frac{g(y-D)}{a_r^2}\right)$$

(3.12)

where:

A_o=the area without excess pressure and a_r is given as:

$$a_r = \sqrt{\frac{E_r \cdot e}{\rho_0 \cdot D}}$$

(3.13)

with:

E_r =   the Young`s modulus of elasticity, [Nm^{-2}]
e =   the pipe wall thickness, [m].

The a_r has the dimension [ms^{-1}] and is in the order of 1400 [ms^{-1}] for most concrete pipes.

Combining these equations yields:

$$\frac{\partial A}{\partial t} + \frac{A}{\rho} \cdot \frac{\partial \rho}{\partial t} = g \cdot A \frac{\partial y}{\partial t}\left(\frac{1}{a_r^2} + \frac{1}{a_0^2}\right) = \frac{gA_0}{a^2} \cdot \frac{\partial y}{\partial t}$$

(3.14)

where:

$$a = \frac{a_0}{\sqrt{1\,a_0^2/a_r^2}}$$

(3.15)

represents the speed of sound in water considering the compressibility of water and the deformation of the pipe wall.

Equation (3.10) can now be written as:

$$\frac{\partial Q}{\partial x} + \frac{Q}{\rho} \cdot \frac{\partial \rho}{\partial x} + \frac{gA_0}{a^2} \cdot \frac{\partial y}{\partial t} = 0$$

(3.16)

The analogy with the continuity equation can thus be maintained in case that the fictitious slot width b_{slot} is specified as:

$$b_{slot} = g \cdot \frac{A_0}{a^2}$$

(3.17)

a is in the order of 1000 [ms⁻¹] for most pipes.

In order to obtain a smooth transition between the free surface flow computations and pressurised flow computations, it is required to apply a "soft" transition between the actual pipe geometry and the fictitious slot. Such a "smooth" transition has been designed based on a series of tests with various slot configurations. The slot configuration thus obtained ensures stable computations without affecting the accuracy significantly. The applied slot width is larger than the theoretical value. The default relation between relative depth and the slot width as implemented in MOUSE is given in Table 3.1.

Table 3.1   Relation between relative depth and slot width

y/D	B_{slot}/D(D=1m)
0.98	0.36
1.00	0.19
1.10	0.0166
1.20	0.0151
1.50	0.0105
>1.50	0.0100

The default slot width can be modified for individual links through the *.ADP file.

3.4   Kinematic Wave Approximation

3.4.1   General

The flow conditions in steep, partly full pipelines are mainly established by the balance between gravity forces and friction forces. Consequently, the inertia and pressure terms in the momentum equation are less dominant. Accelerations are comparably small and the flow is almost uniform, so that the kinematic wave approximation is a reasonable approach.

The momentum equation reduces to:

$$gAI_f = gAI_0 \qquad (3.18)$$

i.e. the friction slope is equal to the bottom slope (uniform flow conditions). In MOUSE, the Manning's formula for uniform flow is used and the momentum equation reads:

$$Q = MAR^{2/3}I_0^{1/2} \qquad (3.19)$$

The kinematic wave is independent of the downstream conditions, meaning that disturbances only propagate downstream. The kinematic wave descrip-

tion can therefore only be applied in cases when the flow is independent of the downstream conditions which is the case in supercritical flow (Froude's number *Fr* > 1).

The analysis of the characteristics of the kinematic wave approximation reveals that a solution obtained for partly filled pipes is physically unrealistic, as the characteristic wave speed $\partial Q/\partial A$ increases with increasing depth in a circular pipe filled for less than 60% and decreases with increasing depth when the pipe is filled for more than 60%. This points that an uncritical use of the kinematic wave approach can lead to incorrect results, caused by an unrealistic deformation of the propagating wave.

The kinematic wave is by nature undamped. The flow rate and the water depth will therefore remain unchanged for an observer moving downstream with the velocity $\partial Q/\partial A$.

Generally, it is not realistic to neglect pressure and inertia terms in the momentum equation in most real flow situations. Therefore, the kinematic wave approximation has to be used with care.

3.4.2   Implementation

The computations of the kinematic wave approximation in MOUSE are facilitated with the so-called 'degree-of-filling' function.

The 'filling' function can be determined from the Manning's formula assuming uniform flow conditions, i.e. $I_f = I_0$:

$$F\left(\frac{y}{D}\right) = \frac{Q}{Q_{full}} = \frac{MAR^{2/3}}{M_{full}A_{full}R_{full}^{2/3}} \tag{3.20}$$

where suffix '*full*' indicates values corresponding to a filled pipe and *y/D* indicates the degree of filling.

This theoretically determined "filling" function has an over-capacity at *y/D* > 0.9.

The "filling" function applied in MOUSE does not include this over-capacity but follows the Manning function up to a value of *y/D* = 0.8, see Figure 3.3.

According to the kinematic wave theory, Q/Q_{full} will not increase further after the pipe runs full, as the pressure grade line is assumed to remain parallel to the pipeline. In reality, however, pressurised flow often gives rise to an increased pressure gradient and thus an increased flow rate. The kinematic wave theory is therefore not suitable for computations of pressurised flow without special adaptations.
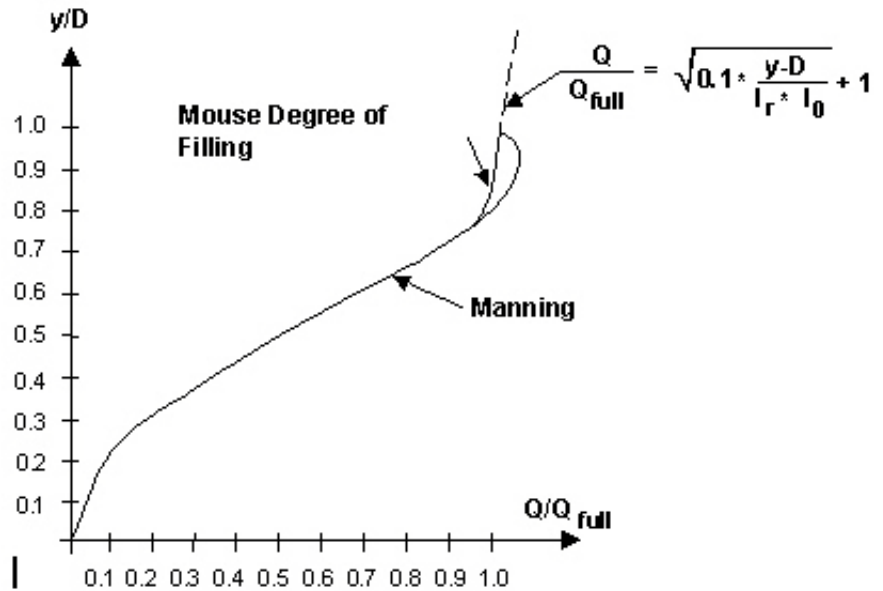
Figure 3.3   The "Degree-of-Filling" function applied in MOUSE

In order to make an approach to pressurised flow, the following assumption has been made: An increase in pressure gradient gives rise to an increased flow rate according to:

$$\frac{Q}{Q_{full}} = \sqrt{0.1 \cdot \frac{y-D}{l_r \cdot l_0} + 1}$$ (3.21)

l_r is the remaining part of the pipe length.

This correction corresponds to an empirical deviation from the kinematic wave theory, so that the pressure grade line is no longer parallel to the pipe slope. 10% of the excess pressure is now used to increase the pressure gradient, see Figure 3.4.
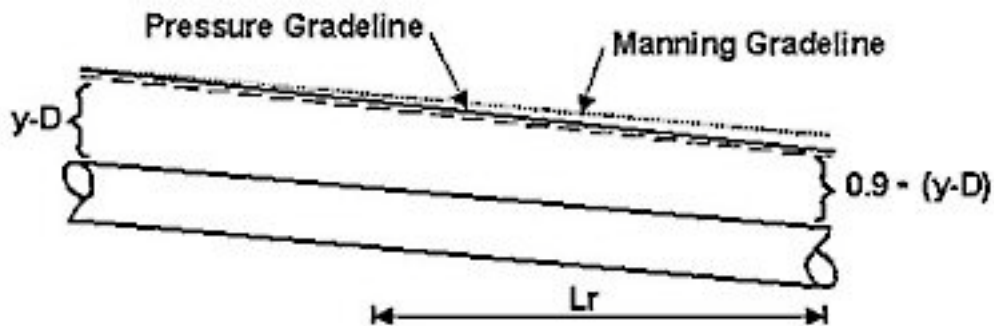
Figure 3.4   The assumption that 10% of the excess pressure is used to increase the pressure gradient

3.5   Diffusive Wave

It was mentioned above that numerical errors in connection with the numerical solution of the kinematic wave equations produce a diffusive (dampened) wave motion. If the pressure term is included in the equation of momentum then a damping term will automatically be included in the equations (the correct solution is a dampened wave motion).

The momentum equation for diffusive wave approximation reads:

$$gA\frac{\partial y}{\partial x} + gAO_f = gAI_0 \qquad (3.22)$$

By retaining the pressure term ($\partial h/\partial x$) in the computation, it is possible to implement the downstream boundary conditions and thus consider backwater effects. The diffusive wave approximation is therefore from a theoretical and practical point of view a better approach than the kinematic wave approximation.

The computational basis for the diffusive wave approximation is in principle identical to the one applied for the dynamic wave approximation for Froude number $Fr > 1$ (supercritical flow). Further more, for stability reasons a moving average in time is applied to the slope of the water surface $\partial h/\partial x$ in order to dampen the short periodic fluctuations. This means that only relatively steady backwater phenomena (compared to the time step) are resolved.

3.6   Dynamic Wave Approximation

3.6.1   General

The general flow equations form the best theoretical foundation for a flow model because the full equation of momentum makes it possible to describe

all forces affecting the flow conditions. However, larger computational load in comparison with the kinematic and diffusive wave approximations involves correspondingly larger CPU time for the same analysis. Additionally, difficulties are present when simulating the supercritical flow conditions.

3.6.2 Supercritical flow simulations with dynamic wave approximation

The full Saint Venant equations (3.1 and 3.2) are applicable in the dynamic wave approximation only for sub-critical flow conditions, i.e. for Froude number $Fr < 1$. In supercritical flow conditions, the equations are reduced to the diffusive wave approximation. In the sub-critical regime, the contribution of the inertia terms ($\partial Q/\partial t$ and $\dfrac{\partial(\alpha Q^2/A)}{\partial x}$) is gradually

taken out by a reduction factor, according to Figure 3.5.
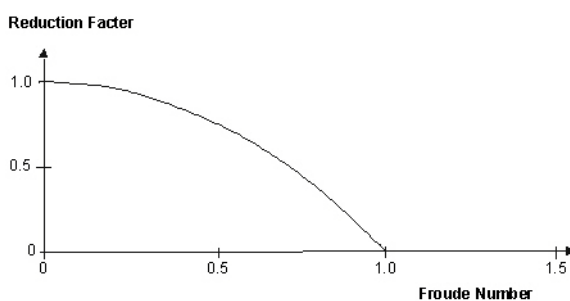
Figure 3.5   Gradual reduction of momentum terms during transition to supercritical flow

Similarly, the differential equation is gradually centred upstream (as the influence of the upstream conditions increases) according to the same function.

3.7 Flow Description in Links - Summary

3.7.1 Inventory

The MOUSE Pipe Flow Model provides a choice between 3 different levels of flow description approximations:

1. **Dynamic wave approach**, which uses the full momentum equation, including acceleration forces, thus allowing correct simulation of fast transients and backwater profiles. The dynamic flow description should be used where the change in inertia of the water body over time and space is of importance. This is the case when the bed slope is small and bed resistance forces are relatively small.

2. **Diffusive wave approach,** which only models the bed friction, gravity force, and the hydrostatic gradient terms in the momentum equation.

This allows the user to take downstream boundary conditions into account, and thus simulate backwater effects. The diffusive wave description ignores the inertia terms and is therefore suitable for backwater analyses in cases where the link bed and wall resistance forces dominate, and for slowly propagating waves where the change in inertia is negligible.

3. **Kinematic wave approach**, where the flow is calculated on the assumption of a balance between the friction and gravity forces. This means that the kinematic wave approach cannot simulate backwater effects. Thus this description is appropriate for steep pipes without backwater effects.

3.7.2   Which Flow Description

Depending on the type of problem, the most appropriate description can be selected. All three approaches simulate branched as well as looped networks.

The dynamic wave description is recommended to be used in all cases except where it can be shown that either the diffusive or kinematic descriptions are adequate.

The diffusive and kinematic wave approximations are simplifications of the full dynamic descriptions. They are implemented to offer improved computational efficiency, but should only be used when the omitted terms have insignificant influence. When there is any doubt it is better to use the full dynamic description or trials should be undertaken to establish the difference between the alternative methods, and advice sought from experienced persons. It is very important to have a solid understanding of the influence of the different terms.

None of the three wave descriptions includes detailed hydraulic descriptions of hydraulic jumps. However, the chosen formulations ensure a correct description upstream and downstream of the jump.

4 Numerical Solution of the Flow Equations in MOUSE Link Networks

4.1 General

The implemented algorithm solves the flow equations by an implicit finite dif-ference method. Setting the numerical scheme into the frame of the Double-Sweep algorithm ensures preservation of the mass continuity and compatibil-ity of energy levels in the network nodes.

The solution method is the same for each model level (kinematic, diffusive, and dynamic).

4.2 Computational Grid

The transformation of Equations (3.1) and (3.2) to a set of implicit finite differ-ence equations is performed on a computational grid consisting of alternating Q- and h-points ("staggered" grid), i.e. points where the discharge Q and water level h, respectively, are computed at each time step (see Figure 4.1). The computational grid is generated automatically by the model, or with user specified number of grid points.

The computational grid for a conduit contains an odd number N of Q and h points, with h points at both ends. The minimum number of computational points N in a conduit is 3, i.e. two h points and one Q point in between. The points are all equally spaced, with a distance x equal to:

$$\Delta x = \frac{l}{N-1}$$

(4.1)

where l is the conduit length.

On the basis of the input data and the specified time step the model automat-ically generates a complete computational grid, based on the velocity condi-tion (see section 4.5 Stability Criteria *(p. 70)*). The velocity used in the calculation is a full-flow velocity, obtained from the Manning formulation assuming completely filled conduit.

If the velocity condition can not be satisfied for the specified simulation time step, which often happens with short and steep pipes, then the model issues a warning, with proposal for a shorter time step, required for the condition to be satisfied.

The grid generated by the model can be altered individually for each conduit, i.e. can be made more dense or sparse, according to the needs of the current application (see documentation on *.ADP file).
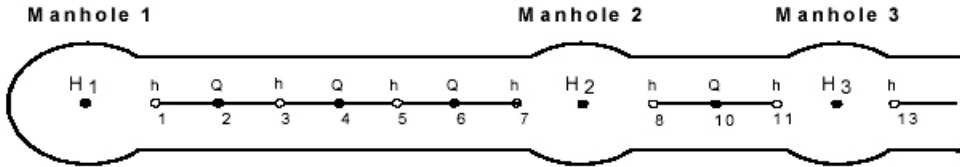
Figure 4.1   A section of the network with Computational Grid.

4.3   Numerical Scheme

The implemented numerical scheme is a 6-point Abbott-scheme (see ref. /2/). The scheme for the method is shown in Figure 4.2.
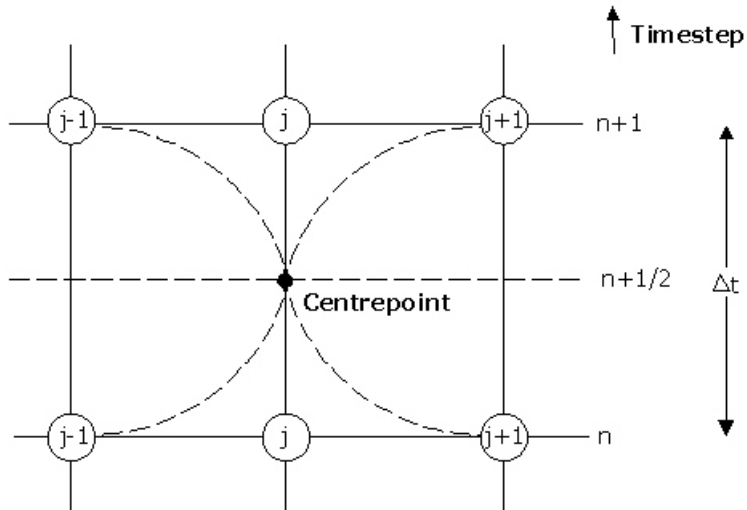
Figure 4.2   Centred 6-point Abbott scheme

The flow equations are approximated by finite differences.

4.3.1   Continuity Equation

In the continuity equation the storage width, b_s, is introduced as:

$$\frac{\partial A}{\partial t} = b_s \frac{\partial h}{\partial t} \tag{4.2}$$

giving

$$\frac{\partial Q}{\partial x} + b_s \frac{\partial h}{\partial t} = 0 \tag{4.3}$$

As only Q has a derivative with respect to x, the equation can be centred at an h-point (see Figure 4.3).
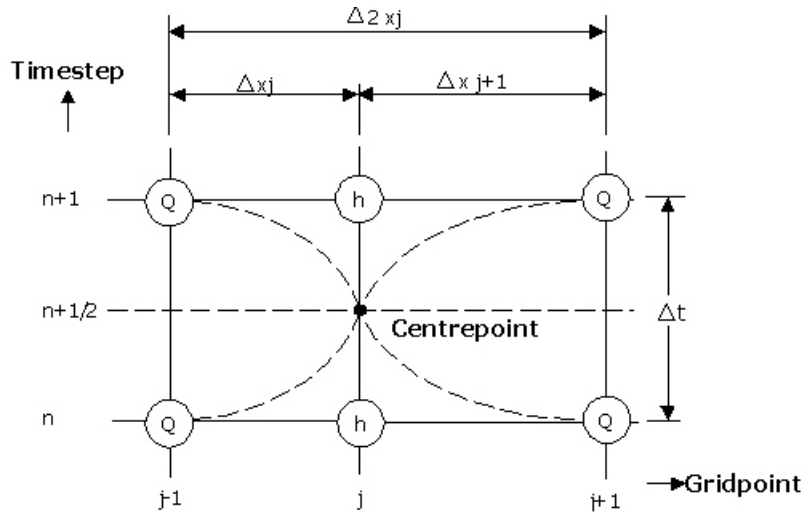
Figure 4.3   Centring of the continuity equation in the Abbott scheme (a generalised scheme). Note that in MOUSE Δx_j and Δx_{j+1} are always equal

The individual derivative terms in Equation (4.3) are expressed by finite difference approximations at the time level, n+½, as follows:

$$\frac{\partial Q}{\partial x} \approx \frac{\frac{(Q_{j+1}^{n+1} + Q_{j+1}^{n})}{2} - \frac{(Q_{j-1}^{n+1} + Q_{j-1}^{n})}{2}}{2\Delta x_j} \tag{4.4}$$

$$\frac{\partial h}{\partial t} \approx \frac{h_j^{n+1} - h_j^{n}}{\Delta t} \tag{4.5}$$

b_s is approximated by:

$$b_s = \frac{A_{o,j} + A_{o,j+1}}{2\Delta x_j} \tag{4.6}$$

where:

$A_{0,j}$	=	the surface area between grid points $j-1$ and j
$A_{0,j+1}$	=	the surface area between grid points j and $j+1$
$2\Delta x_j$	=	distance between points $j-1$ and $j+1$

Substituting for the finite difference approximations in Equation (4.3) and rearranging gives a formulation of the following form:

$$\alpha_j Q_{j-1}^{n+1} + \beta_j h_j^{n+1} + \gamma_j Q_{j+1}^{n+1} = \delta_j \tag{4.7}$$

where α, β and γ are functions of b_s and δ and, moreover, depend on Q and h at time level n and Q on time level $n+\frac{1}{2}$.

4.3.2 Momentum equation

The momentum equation is centred at Q-points as illustrated in Figure 4.4.

The derivatives of Equation (3.7) are expressed as finite difference approximations in the following way:

$$\frac{\partial Q}{\partial t} \approx \frac{Q_j^{n+1} - Q_j^n}{\Delta t} \tag{4.8}$$

$$\frac{\partial \left(\alpha \frac{Q^2}{A} \right)}{\partial x} \approx \frac{\left(\left[\alpha \frac{Q^2}{A} \right]_{j+1}^{n+\frac{1}{2}} - \left[\alpha \frac{Q^2}{A} \right]_{j-1}^{n+\frac{1}{2}} \right)}{2 \Delta x_j} \tag{4.9}$$

$$\frac{\partial h}{\partial x} \approx \frac{\dfrac{h_{j+1}^{n+1} + h_{j+1}^n}{2} - \dfrac{h_{j+1}^{n+1} + h_{j-1}^n}{2}}{2 \Delta x_j} \tag{4.10}$$
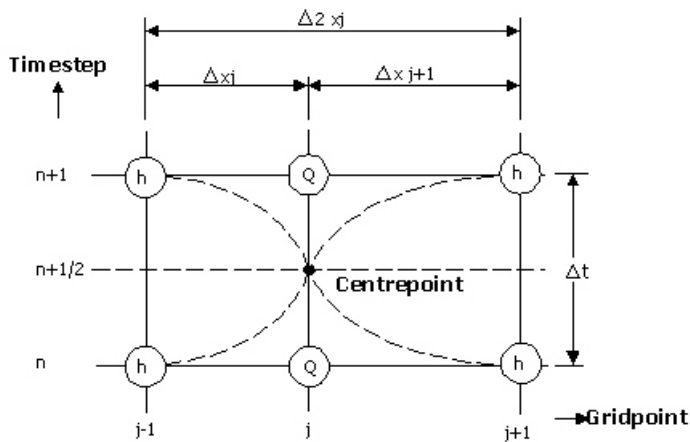
Figure 4.4   Centring of the momentum equation in the Abbott scheme

For the quadratic term in Equation (4.9), a special formulation is used to ensure the correct sign for this term when the flow direction is changing during a time step:

$$Q^2 = f \cdot Q_j^{n+1} \cdot Q_j^n - (f-1) \cdot Q_j^n \cdot Q_j^n \qquad (4.11)$$

where

$$f = \frac{Q_j^{n+1/2} \cdot Q_j^{n+1/2} - Q_j^n \cdot Q_j^n}{Q_j^n \cdot (Q_j^{n+j} - Q_j^n)} \qquad (4.12)$$

As standard, f is set to 1.0.

With all the derivatives substituted by finite difference approximations and appropriately rearranged, the momentum equation can be written in the following form:

$$\alpha_j h_{j-1}^{n+1} + \beta_j Q_j^{n+1} + \gamma_j h_{j+1}^{n+1} = \delta_j \qquad (4.13)$$

where

$$\begin{aligned}
\alpha_j &= f(A) \\
\beta_j &= f(Q_j^n, \Delta t, \Delta x, M, A, R) \\
\gamma_j &= f(A) \\
\delta_j &= f(A, \Delta x, \Delta t, \alpha, q, v, \theta, h_{j-1}^n, Q_j^{n+1}, Q_j^n, h_{j+1}^n, Q_{j+1}^{n+1})
\end{aligned} \qquad (4.14)$$

4.4 The "Double Sweep" Algorithm

4.4.1 "Branch matrix"

As shown earlier, the continuity equation and momentum equation can be formulated in a similar form (compare Equation (4.7) and Equation (4.13)).

Using, instead of h and Q, the general variable, Z, (which thus becomes h in grid points with odd numbers and Q in grid points with even numbers), the general formulation will be:

$$\alpha_j Z_{j-1}^{n+1} + \beta_j Z_j^{n+1} + \gamma_j Z_{j+1}^{n+1} = \delta_j \qquad (4.15)$$

Writing the appropriate equation for every grid point, a system of equations is obtained for each conduit (branch) in the network, constituting the 'branch coefficient matrix', as illustrated in Figure 4.5.

Applying a local elimination, the branch coefficient matrix can, in principle, be transformed as shown in Figure 4.6 below. It is thus possible to express any water level or discharge variable within the branch as a function of the water levels in the upstream and downstream nodes (e.g. manholes) H_1 and H_2, i.e.:

$$h = h(H_1, H_2) \tag{4.16}$$

and similarly:

$$Q = Q(H_1, H_2) \tag{4.17}$$
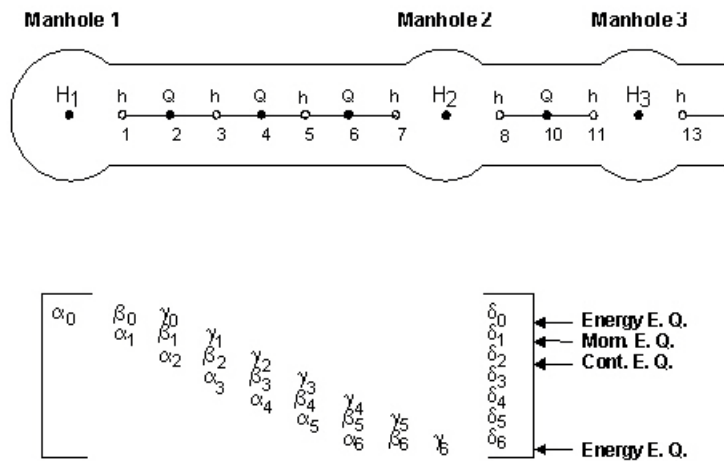
Figure 4.5   "Branch" matrix, with coefficients derived from the node energy level, momentum and continuity equations
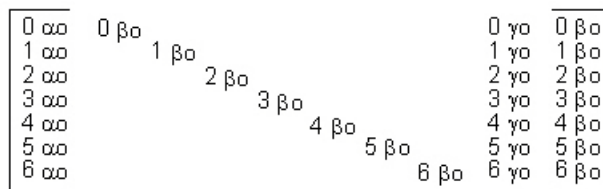
Figure 4.6   "Branch" matrix after local elimination

The continuity equation around a node can in principle be expressed as:

$$ah_{node}^{n+1} + bh_{branch_1}^{n+1} + cQ_{branch_1}^{n+1} + dh_{branch_2}^{n+1} + eQ_{branch_2}^{n+1} + \dots = z \tag{4.18}$$

where, *a..z* are quasi-constants. If Equation (4.15) is substituted herein, a global relation can be obtained:

$$AH_1 + BH_2 + ... = Z \qquad (4.19)$$

where *A*, *B*, ... to *Z* are quasi constants.

Equation (4.19) shows that the water level in a node can be described as a function of the water levels in the neighbouring nodal points. It is therefore possible to set up a 'nodal point matrix' at each time step using the coefficients from Equation (4.19) and the solution to the matrix yields, by backward substitution, the water levels in all nodal points at the next time step.

Figure 4.7 shows an example with 8 nodal points and 9 branches.
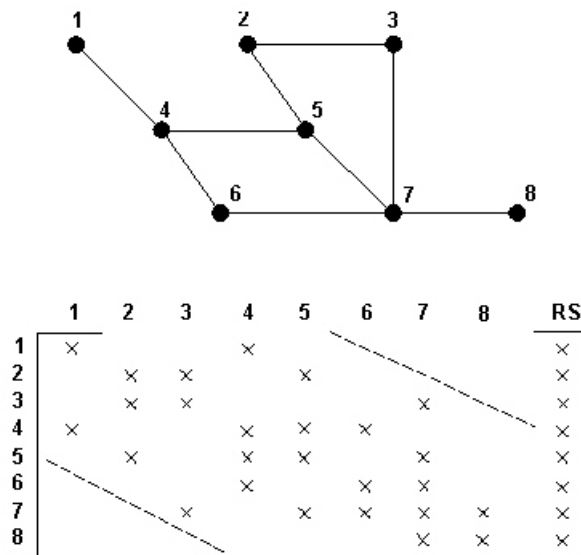
Figure 4.7   Principle of a "nodal" matrix for a system with 8 nodes and 9 branches

The crosses in the matrix symbolise coefficients, meaning that, for instance, the water level in node 4 can be expressed as a function of the water levels in nodes 1, 5 and 6. When the nodal point matrix has been solved, the solution in the branches is found by backward local elimination.

The bandwidth of the nodal point matrix, as indicated by the stippled lines, depends on the order in which the nodal points are defined. The bandwidth of the matrix in Figure 4.7 is equal to 5. The computational time required for solution of the nodal point matrix depends on the bandwidth size, and sharply increases with increasing bandwidth.

In order to minimise the computational time, an automatic minimisation of the bandwidth is performed by internal perturbation of the nodal points. The bandwidth displayed in Figure 4.7 (for the network with 8 nodal points and the 9 branches) could be reduced to 4 as shown in the matrix in Figure 4.8.

Figure 4.8   Minimised matrix band width

4.5   Stability Criteria

A criterion for a stable solution of the finite difference scheme is given by the Courant condition:

$$C_r = \frac{\Delta t(v + \sqrt{gy})}{\Delta x}$$

(4.20)

where:

v=mean flow velocity, [ms^{-1}]

Δt=time step, [s]

Δx=distance between computational points in the conduit, [m]

y=water depth, [m].

Theoretically, the implemented numerical scheme is unconditionally stable for all Courant numbers. In practice, however, this is restricted, because the numerical implementation and the accuracy criteria impose some additional limitations.

The most conservative condition for a correct and stable solution of the implemented finite difference scheme is the velocity condition:

$$v \cdot \Delta t \le \Delta x$$

(4.21)

The automatically generated computational grid fulfils this condition.

4.6 Optimising the Simulation Time Step Δt

The computational efficiency of any discrete-time numerical simulation algorithm is highly dependent on the time step applied in the simulations. In turn, the feasible time step in a concrete situation depends on, apart from the inherent performance properties of the computational scheme, the dynamics of the flows in the simulated network. It is therefore desirable to optimise the algorithm so that in conditions of variable flow dynamics as usually occur during the simulated interval, the total computational effort is minimised, while preserving stable and accurate computations.

MOUSE optimises the simulation time step by:

- The automated self-adaptive time step variation. This is controlled by the actual hydraulic and operational conditions within the entire model area throughout the numerical simulation

This concept can be applied in connection with the Dynamic and Diffusive flow descriptions while it cannot be used with the Kinematic flow description.

In this context, it is important to note that a constant time step is simply a restricted case of these concepts.

4.6.1 Automated, Self-adaptive Time Step Variation

The automated, self-adaptation of the simulation time step is performed during the running simulation. Such on-the-fly calculation of the time step is performed through a three-step procedure:

- Before the actual time step is taken, a preliminary value of the time step is calculated, on the basis of the following:

    The instantaneously time step is increased by a user-specified fraction (the time step acceleration). Acceptance of this time step is validated through checking the resolution of boundary conditions and pump operations (see below). Finally, the suggested time step is validated with respect to user-specified minimum and maximum values. The minimum and maximum values and acceleration factors are specified as a part of the simulation configuration. If the maximum and minimum values of *dt* are equal, the program will use a constant time step.

- The preliminary hydrodynamic solution is calculated with the preliminary time step value.

- Based on an assessment of the preliminary solution, a judgement is made whether the used time step is acceptable or not. The user has the opportunity to specify numerous different limitation factors, such as a maximum allowed variation in the water level in grid points, a maximum allowed variation in the courant number, etc. A list of all possible limiting factors is given below. If any of these criteria are exceeded, i.e. if the generated variation is too large, then a revised solution is calculated. The revised solution is obtained as a linear interpolation between the last two simulation results (the previous time step solution and the solution with preliminary time step), so that all specified criteria are fulfilled.

The different criteria which control the variation in the time step are outlined below. The user has the option to modify the individual criteria through variation in the parameters. All of these parameters must be defined in the DHIAPP.INI file.

4.6.2 Criteria Controlling the Self-adaptive Time Step Variation

Resolution of the Boundary Conditions

The time step is limited by the excessive errors generated due to the difference in the boundary time series resolution. In case of relatively fine resolution of boundary time series, application of long time steps may e.g. cause volume errors. The maximum allowed error in the boundary conditions is given by :

$$\varepsilon < QacceptLimitRel \cdot Bvar \tag{4.22}$$

where ε is the largest error between the given and simulated boundary conditions (see Figure 4.9), *Bvar* is the value of the given boundary conditions and *QacceptLimitRel* is a user specified value given in the DHIAPP.INI file.
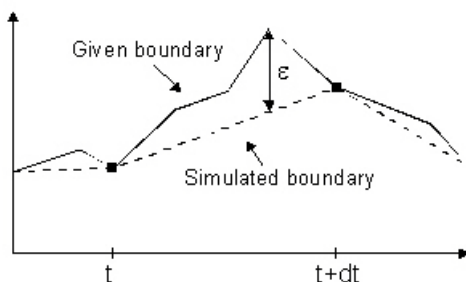

Figure 4.9   Resolution of the boundary conditions

The boundary resolution criteria is tested on all time series defined as boundary or results from a runoff simulation (the *.CRF file). However, the test is

only applied to boundary conditions which are larger than *QlowLimitM3s* , a minimum flow threshhold value.

The default value of *QacceptLimitRel* is 0.1 and *QlowLimitM3s* 0.01.

Variation in the Operation of the Pump Flow

The variation in the pump flow through one time step is limited by:

$$\Delta Q < MaxPumpFlowVar \cdot Q \tag{4.23}$$

where ΔQ is the variation in the pumped flow, Q is the current value of the pumped flow and *MaxPumpFlowVar* is the user specified maximum relative variation.

The default value of *MaxPumpFlowVar* is 0.1 which corresponds to a 10% maximum variation in the pumped flow during one time step.

It should be noted that this test also implies that the simulation is always decelerated down to the minimum time step whenever a pump is switched ON or OFF.

Variations in the water level in grid points

The variation of the water level in all H-grid points is limited by the following functions:

$$\Delta H < \sqrt{WaterLevDiffMaxRel \cdot H} \tag{4.24}$$
$$\text{for} \quad (H < WaterLevDiffMaxRel, H1 > H0)$$

$$\Delta H < H \text{ for } (H < WaterLevDiffMaxRel, H1 < H0) \tag{4.25}$$

$$\Delta H < WaterLevDiffMaxRel \text{ for } H > WaterLevDiffMaxRel \tag{4.26}$$

where H is the relative depth (the water depth divided by the height, e.g. by diameter for circular pipes), $H0$ is the relative depth before the attempted time step and $H1$ is the relative depth at the end of the time step. ΔH is the difference in the relative depth through the time step. The *WaterLevDiffMaxRel* value can be user-controlled from DHIAPP.INI file. If limitation is violated at any H-point in the model, then the obtained solution is scaled down with respect to *dt*.

The default value of *WaterLevDiffMaxRel* is 0.3, which corresponds to a maximum relative change of 30 %.

Variation of Cross-Section Parameters

The variation of cross-section parameters A, $R^{2/3}$ and B, where A is the cross section area, R is the hydraulic radius and B the width of water surface can be included as additional criterion for limiting the simulation time step. Whether the check on the cross-section parameters is to be activated or not

is specified through the variable *Crosscheck* in the DHIAPP.INI file (the value 0 means that this is de-activated, while the values 1 or 2 mean that the check is activated in one of the two available variants). If the check on the cross-section parameters is activated, then it is carried out in all H-grid points.

The variation in the three cross-section parameters is limited by:

$$\Delta X < MaxVarCrossCons\tan t \cdot Max(X) \tag{4.27}$$

where the variable *X* is one of the three cross-section variables and the meaning of Max(*X*) depends on the value of *Crosscheck*. If *Crosscheck* is given as 1 then Max(*X*) is the maximum value of the actual parameter over the cross section, while a value of *Crosscheck* which is equal to 2 means that Max(*X*) is given as the actual value of the respective cross-section parameters. However, the check is carried out only if the relative depth in the cross-section is larger than the variable *CrossLowDepthLimit*. The check of these limitations is carried out at the end of a time step simulation. If limitations are violated then the solution is scaled down with respect to *dt*.

The default value of *MaxVarCrossConstant* is 0.03, if *Crosscheck* is 1 and *CrossLowDepthLimit* is 0.04.

Variation in Courant Number

In the dynamic flow conditions, the Courant number (see section 4.5 Stability Criteria *(p. 70)*) is continuously changing from time step to time step. In order to avoid stability and accuracy problems, the Courant number is limited by:

$$C < MaxCourant, \text{ where } C = \frac{V \cdot dt}{dx} \tag{4.28}$$

V is flow velocity and *dx* the distance between two computational grid points.

Check of this limitation is carried out after the simulation of a time step. If the limitation is violated the solution is scaled down with respect to *dt*.

Recommended value of *MaxCourant* (specified in DHIAPP.INI file) is 20 – 60.

Weir oscillations

If the storage volume in one of the nodes connecting a weir is small, weir oscillations might occur for free flow conditions. This phenomenon results in a continuous change in flow direction over the weir until the instability is dampened. In order to avoid this situation, a criterion related to the change in water levels between up- and downstream nodes around the weir is implemented. The criterion relates to *dt* by:

$$dt_{possible} \cdot (\Delta H^n + \Delta H^{n+1}) = dt \cdot (\Delta H^n - 0.02) \tag{4.29}$$

where ΔH is the difference in water level between the two nodes connected to the weir and n corresponds to the time step level. The absolute allowed change of 0.02 m is hard-coded in the program and cannot be controlled by the user.

4.7   Mass Continuity Balance

Theoretically, what concerns the mass continuity balance, the applied computational scheme is inherently conservative for prismatic conduits with vertical walls. In practical applications, the continuity balance may be jeopardised in a number of situations, such as:

- Relatively sharp changes of surface width due to rapid changes of water depth or a sharp change of cross-section shape with depth. This may be e.g. the case at relatively small depths in circular pipes and in arbitrary cross sections

- Sharp changes in surface area of basins

- Surcharge of manholes

- Etc.

The scale of the problem is usually related to the length of the simulation time step.

4.7.1   Improved Continuity Balance for Links

In order to reduce the amount of water generated in conduits due to the changes of surface width as function of water depth, i.e. to improve the continuity balance, the Taylor expansion of the general continuity equation (3.1) has been applied. Since the surface width is assumed to be constant during two time steps, the continuity equation can be rearranged as:

$$\frac{1}{w}\frac{\partial Q}{\partial x} + \frac{\partial h}{\partial t} = 0 \tag{4.30}$$

where h is the water level (m) and w is the surface width (m).

The term $\dfrac{1}{w}\dfrac{\partial Q}{\partial x}$ in the equation above can be expanded in a Taylor series as:

$$\frac{1}{v}\frac{\partial Q}{\partial x} \approx \left(\frac{1}{w}\frac{\partial Q}{\partial x}\right)^n - \theta\left(\frac{1}{w^2}\right)^n\frac{\partial w}{\partial h}\left(\frac{\partial Q}{\partial x}\right)^n\Delta h + \theta\left(\frac{1}{w}\right)^n\left(\frac{\partial Q^{n+1}}{\partial x} - \frac{\partial Q^n}{\partial x}\right) \tag{4.31}$$

where θ represents the time centering of the numerical scheme and n and $n+1$ refer to the simulation time steps.

This modification is applicable only for conduits with relatively smooth changes of the surface width. As the width for arbitrary pipes and pipes from

the cross-section database may vary in a very unpredictable way, the Taylor expanded equation is only applied to standard pipes.

4.7.2   User Defined Minimum Water Depth

Further means of controlling the volume continuity balance for links with no or little water are provided as user-controlled minimum water depth for links running dry or with very little flow. The default minimum water depth can be modified in the DHIAPP.INI file. In this file two parameters can be changed:

- **BRANCH_MIN_H_REL=20**. This is the relative minimum water depth (in promille of the characteristic dimension) in a link

- **BRANCH_MIN_H_ABS=20**. This is the absolute minimum water depth (mm) in a link.

The minimum water depth in a link will be set to **BRANCH_MIN_H_REL,** calculated as promille of the link size (e.g. pipe diameter or height of the open channel), but never larger than **BRANCH_MIN_H_ABS** mm. In the presented example, the minimum water depth is set to 20 promille of the link size, but with a maximum of 20 mm. This means that for links smaller than 1 meter the minimum water depth is set to 20 promille of the link size. For links larger than 1 meter the minimum water depth is kept at 20 mm, independently of the link dimensions.

5 Initial Conditions

The hydrodynamic computation is started from the flow conditions in the systems specified for time *t* = 0. MOUSE provides two different options for establishment of proper initial conditions.

5.1 Default Initial Conditions

MOUSE automatically specifies the initial conditions, establishing a default initial water depth equal to 0.5% of the characteristic dimension of the conduit (diameter for circular pipes), but not more than 0.005 m, and flow rates are calculated based on the Manning formulation for uniform flow.

In case of dry weather flow applications, the volume of artificially generated water may be significant compared to the dry weather flows. This may compromise the volume balance the analysis. For such cases, the default initial depth can be reduced by setting the parameters *BRANCH_MIN_H_REL* (controls the initial depth relative to the conduit size) and *BRANCH_MIN_H_ABS* (controls the absolute depth of the initial water depth) to appropriate values (in the DHIAPP.INI file).

If there are outlets in the system with initial water level specified higher than the outlet bottom, a horizontal water surface is assumed extending inside the system, until the point in the pipe system where the water level coincides with the bottom level (see Figure 5.1).
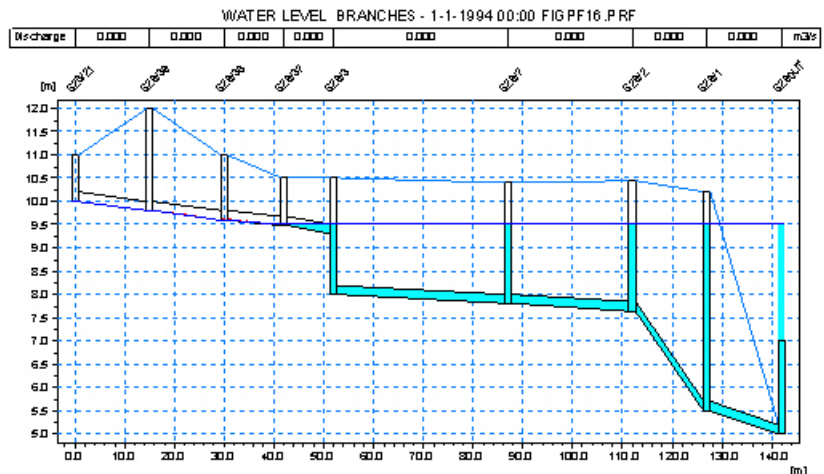
Figure 5.1 Initial conditions with backwater outlet.

5.2   Initial Conditions provided by Hotstart

Realistic initial conditions can be specified by taking the water levels and discharges from previously calculated result file. Flow conditions at any time level contained in the interval covered by the result file can be chosen as initial condition.

The result file used as a HOTSTART file has to be complete, i.e. water levels and flows at all computational points have to be saved.

6   Boundary Conditions

Unique solution of the flow equations requires appropriate set of boundary conditions. Flow equations are solved for each conduit between two nodes, and the boundary conditions are required at both end of the conduit, at each time step throughout the computation.

In some situations boundary conditions are specified as unique relations of two flow variables (e.g. stage/discharge relation), i.e. as hydraulic boundaries in certain points. These are defined as functions, i.e. as a part of the system description.

In other cases, proper boundary conditions are constructed by the model as a consequence of current flow situation and of various user-specified disturbances in form of e.g. adding or extracting water, controlling the flow, adding energy (pumping) or as effect of external water level. These disturbances may be constant (stationary) or time-variable.

By default, MOUSE supplies all necessary boundary conditions, founded on the topology and geometry of the system. Therefore, the simulations can be run even if no boundary conditions of the other type are specified by the user.

With respect to the volume balance in the system, two groups of boundary conditions can be distinguished:

1. External boundary conditions, describing the interaction of the modelled system with its surroundings

2. Internal boundary conditions, describing relations between certain parts of the model.

The **external** boundary conditions comprise the following:

At manholes and structures:

1. Constant inflow or extraction, Q = const.,
2. Time variable inflow or extraction, $Q = Q(t)$,
3. Computed inflow hydrograph, $Q = Q(t)$,
4. Weir discharging out of the system, $Q = Q(H)$,
5. Pump discharging out of the system, $Q = Q(H)$.

Application of negative inflows (extraction) should be done with due care, because extraction of more volume than the system can supply would end up with error in computations.

At outlets:

1. Constant outlet water level, H = const.,
2. Time variable outlet water level, $H = H(t)$,

3. *Q/H* relation at the outlet, *Q = Q(H)*.

Internal boundary conditions can be defined as follows:

At manholes and structures:

1. Weir discharging to another manhole or structure, *Q = Q(H)*, where *H* stands for energy level above the weir crest in case of a free overflow, and for difference of energy levels upstream and downstream of the weir in case of a submerged overflow.

If an alternative formulation for the weir is specified with a user-specified *Q/H* relation, such conditions should be provided that the overflow is always free, i.e. that holds the unique relation between the water level and the flow.

2. Pump discharging to another manhole or structure, *Q = Q(H)* or *Q = Q(ΔH)*, where *H* stands for water level in the manhole or structure, and *ΔH* level difference between the two manholes or structures associated with the pump.

Some of the listed boundary conditions are illustrated in Figure 6.1.
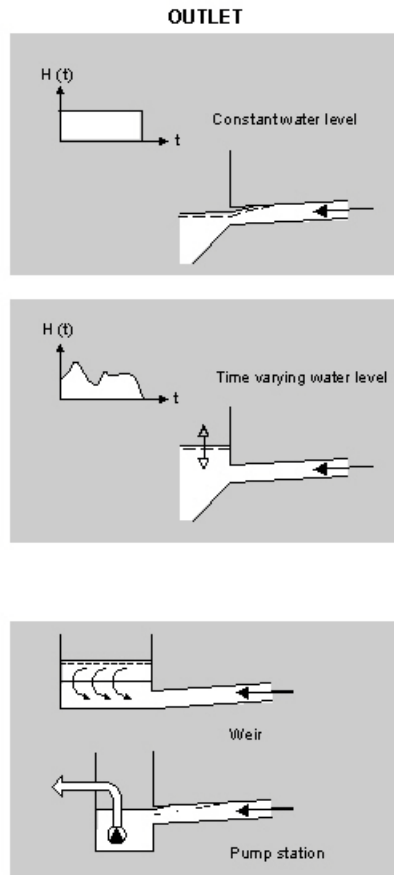
Figure 6.1   Supplying Boundary Conditions – Examples (to be continued)

INFLOW
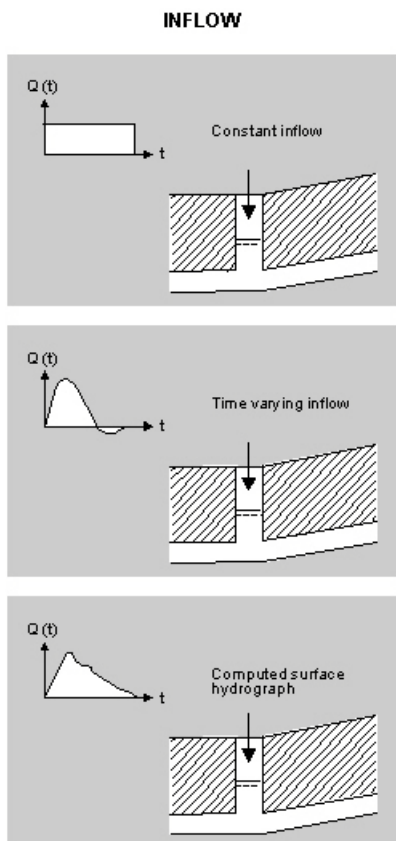
Figure 6.2   Supplying Boundary Conditions – Examples (continued)

7   Flow Resistance

7.1   Friction Losses in Free-Surface Flow Links

7.1.1   Numerical Description

Head losses caused by the resistance in free-surface flow links are introduced as a friction slope term into the momentum equation (see section 3.2 Implementation of the Saint Venant Equations in MOUSE *(p. 52)*). The friction slope I_f is equal to the slope of the energy grade line and is defined as:

$$I_f = \frac{\tau}{\rho g R}$$ (7.1)

where:

τ =   tangential stress caused by the wall friction, [Nm^{-2}],

ρ =   density of water, [kgm^{-3}],

R =   hydraulic radius, [m], (= A/P, where P is the wetted parameter).

The friction slope can be derived as a function of an appropriate combination of the flow parameters (Q, A and R) and the water and conduit wall properties (υ, k).

Generally, the friction slope can be expressed as:

$$I_f = f \cdot Q^2$$ (7.2)

where f is a generalised friction factor. By these means, the friction slope is explicitly determined as a function of instantaneous values of local flow parameters.

A more stable formulation is achieved through an implicit description of the friction term. It is derived from a variational principle at a grid point j as:

$$I_{fj}^{n+\theta} = I_{fj}^{n} + \theta dI_{fj} = (1-\theta)I_f^n + \theta I_f^{n+1}$$ (7.3)

This results in:

$$I_{f_j}^{n+\theta} = I_{f_j}^n + \theta dI_{f_j} \tag{7.4}$$

$$= f_j^n (Q_j^n)^2 + \theta dI_{f_j}$$

$$= f_j^n (Q_j^n)^2 + \theta \left[2 f_j^n (Q_j^n)^2 + (Q_j^n)^2 \left(\frac{df}{dh} \right)_j^n \Delta h_j \right]$$

The coefficient θ determines the time weighting of the scheme. For stability reasons the coefficient should be above 0.5. The recommended (also default) value is 1.0, i.e. a fully forward time weighting of the scheme.

MOUSE provides an optional choice between the explicit and implicit flow resistance description through the DHIAPP.INI file (see relevant documentation). The explicit description is selected per default.

7.1.2 The Friction Resistance Described by the Manning Formula

The "classic", explicit application of the Manning's formula reads as:

$$I_f = \frac{Q|Q|}{M^2 A^2 R^{4/3}} \tag{7.5}$$

with the friction factor:

$$f = \frac{1}{M^2 A^2 R^{4/3}} \tag{7.6}$$

where M is the Manning number, A the area, and R the hydraulic radius.

Usage of the $Q|Q|$, instead of $Q2$ facilitates computations of the reverse flow.

The Manning's number M (or $n = 1/M$) is the parameter used as a measure of the conduit's wall roughness. Default values are given in section 2.2.2 Specification of a Link *(p. 14)*.

The implicit formulation of the Manning's formula is obtained by the differentiation of f with respect to h, which results in:

$$\frac{\partial f}{\partial h} = -2 \frac{f}{M} \frac{\partial M}{\partial h} - 2 \frac{f}{A} \frac{\partial A}{\partial h} - \frac{4}{3} \frac{f}{R} \frac{\partial R}{\partial h} \tag{7.7}$$

and substituting the derivative into the Equation (7.4).

7.1.3   Depth-variable Manning coefficient

Per default, MOUSE assumes a constant Manning's number over the link section height. However, in real situations conduit wall roughness often changes with water depth, because different parts of the link cross section are exposed to quite different flow conditions during its lifetime. This introduces difficulties in fitting the computed stage-discharge curve, based on a single *M* value specified for a link, with the actual, measured stage-discharge relation. This is usually related to old systems, where significant sediment deposits and pipe-wall erosion are present.

The MOUSE Pipe Flow Model accepts a specification of a non-linear variation of Manning number with relative elevation (water depth in the conduit). Three parameters define the Manning's number variation: bottom value, full flow value and a non-linear exponent. Intermediate values are calculated by a general expression:

$$M_{act} = M_{bott} + (M_{top} - M_{bott}) \cdot \left(\frac{y}{D}\right)^{\exp} \tag{7.8}$$

where:

M_{act}	=	calculated Manning's number,
M_{bott}, M_{top}	=	Manning's numbers specified for the conduit bottom and top, respectively,
exp	=	Manning's number variation exponent, default,
y/D	=	the relative water depth in a conduit.

The formula is used for relative depths h/D in the interval 0.0 - 1.0. For relative depth > 1.0 the Manning number is set to the Manning$_{top}$ value.

The variation between Manning$_{bot}$ and Manning$_{top}$ is controlled by the "Variation Exponent". The variation of the Manning number in relative terms is illustrated in Figure 7.1. An example of the variation is shown in Figure 7.2 with Manning M values.
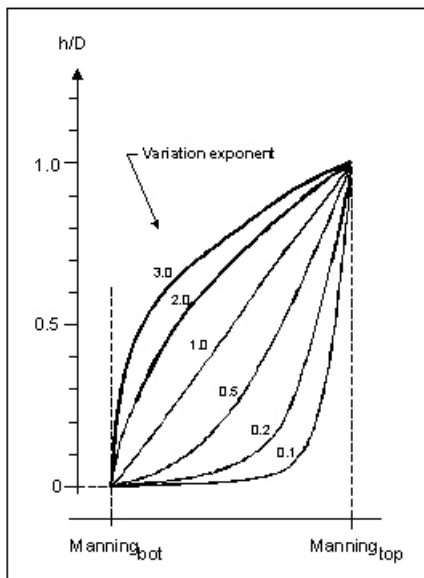
Figure 7.1   Relative variation of the Manning number with relative depth.

h/D	Manning					
1.100	90.000	90.000	90.000	90.000	90.000	90.000
1.000	90.000	90.000	90.000	90.000	90.000	90.000
0.900	89.686	89.374	88.461	87.000	84.300	81.870
0.800	89.338	88.691	86.833	84.000	79.200	75.360
0.700	88.949	87.934	85.100	81.000	74.700	70.290
0.600	88.506	87.086	83.238	78.000	70.800	66.480
0.500	87.991	86.117	81.213	75.000	67.500	63.750
0.400	87.373	84.977	78.974	72.000	64.800	61.920
0.300	86.597	83.580	76.432	69.000	62.700	60.810
0.200	85.540	81.743	73.416	66.000	61.200	60.240
0.100	83.830	78.929	69.487	63.000	60.300	60.030
0.000	60.000	60.000	60.000	60.000	60.000	60.000
Exponent:	0.1	0.2	0.5	1.0	2.0	3.0

Figure 7.2   Variation of the Manning M for Manning$_{bot}$=60 and Manning$_{top}$=90 with different values of the variation exponent.

The Manning number variation is specified through the ASCII file *.ADP. The specified Manning numbers in the *.ADP file must follow the selected option for the Manning number convention. Syntax of the format of the '*.ADP' files must be as shown in the 'DHIAPP.INI and *.ADP Reference Manual'.

The lines of the '*ADP' file related to the Manning number variation may be easily compiled by copy-and-paste operations from the MOUSE650.OUT file. This ASCII file is generated by every computation with the MOUSE Pipe Flow Model.

Before using the '*.*ADP*' file, the Manning number parameters for the selected lines must be modified, i.e. values for bottom and top of pipe Manning numbers and possibly the variation exponent must be adjusted for the pipes or canals where varying Manning numbers are to be used.

7.1.4   Colebrook - White Formula for Circular Pipes

In 1939, Colebrook and White derived an approximate formula which unifies the description of the turbulent flow in both rough and smooth circular pipes. This formula is extensively used for the computation of flow resistance in predominantly full-flowing pipe networks.

According to Colebrook and White, the friction factor *f* is computed iteratively, using one of the several formulations known from the literature. The formula implemented in MOUSE reads:

$$\sqrt{\frac{2}{f_{cw}}} = cw_1 + cw_2 \cdot \ln\left(\frac{cw_3}{Re}\sqrt{\frac{2}{f_{cw}}} + cw_4 \cdot \frac{k}{R}\right) \tag{7.9}$$

where:

k	=	the equivalent wall roughness [m],
R	=	the hydraulic radius,
Re	=	the Reynolds number,

cw_1, cw_2, cw_3, cw_4 = empirical constants.

The default values of the constants cw_1-$cw4$ are:

cw_1 =	6.4
cw_2 =	-2.45
cw_3 =	3.3
cw_4 =	1.0

The default values can be modified through DHIAPP.INI file.

The actual friction slope is calculated by using the following relation:

$$I_f = f_{cw} \cdot \frac{Q^2}{2gA^2R} \Rightarrow f = \frac{f_{cw}}{2gA^2R} \tag{7.10}$$

The Colebrook -White friction resistance can only be used if an implicit friction formulation is activated.

Use of the Colebrook-White formula must be restricted to circular pipes only. Also, the Colebrook-White formula is fully valid for full-flowing pipes.

7.1.5 Hazen-Williams Equation

The Hazen-Williams equation is an empirical formula which relates the flow of water in a pipe with the physical properties of the pipe and the pressure drop caused by friction. It is used in the design of water pipe systems such as fire sprinkler systems, water supply networks, and irrigation systems. The Hazen-Williams equation has the advantage that the coefficient C is not a function of the Reynolds number, but it has the disadvantage that it is only valid for water and it not able to account for temperature or viscosity.

$$Q = k \cdot C \cdot A \cdot R^{0,63} \cdot S^{0,54} \qquad (7.11)$$

where:

k = is a conversion factor for the unit system (k = 1.318) for US customary units, k = 0.849 for SI units),
C = is the roughness coefficient,
R = is the hydraulic radius,
S = is slope of the energy line (head loss per length of pipe)

7.2 Head Losses in Manholes and Structures - Introduction

The general flow equations are valid only for continuous conduits where, in principle, the only resistance to the flow originates from the bottom and side-wall friction. Hydraulic conditions in nodes, i.e. at manholes and structures take the role of boundary conditions for computation of the flows in the conduits. In turn, hydraulic conditions in a node depend on the flows in the inlet and outlet conduits.

These hydraulic conditions, expressed in terms of the energy conservation principle, are calculated as water levels and velocity heads. The calculation is based on the mass continuity and formulation of more or less advanced energy relation between the node and the neighbouring links, with inclusion of some energy losses caused by local flow disturbances at different locations in the node.

The implemented solution ensures that mutual dependence of the flows in links and hydraulic conditions in nodes are correctly resolved, even for complex branched and looped conduit networks.

Energy losses in junctions are of the same order of magnitude as those caused by the pipe wall friction. Knowledge about the magnitude of these energy losses, based on experimental data, is very limited, but some theoretical results are available (e.g. ref. /3/). Importance of a detailed evaluation of these losses is related to the relative length of the links (l/D), and grows with relative shortening of the conduits.

7.3 'Standard' MOUSE Solution (F.A. Engelund)

A simplified computational model for energy losses in junctions implemented in MOUSE is based on F.A. Engelund's energy loss formulae (see ref. /5/). Furthermore, a critical depth formulation, with approximation of critical flow conditions, is used in MOUSE for simulation of a free inlet to a manhole.

7.3.1 Head Loss at the Node Inlet

It is assumed that the water levels in the inlet conduit and in the manhole or structure are the same. This assumption implies that the energy loss of the flow entering and expanding in the node amounts to the difference of the velocity heads in the inlet conduit i and the node m, respectively:

$$\Delta E_i = \frac{v_i^2 - v_m^2}{2g}$$

(7.12)

Essentially one-dimensional analysis in MOUSE relies on this simplification also in nodes with multiple inlet and outlet conduits, i.e. where mixing of flows of different energy levels occurs. Therefore, in some extreme cases, where head losses in nodes play a crucial role for the correct solution, it is advisable to perform a more detailed analysis, in order to assess the approximation errors inherent to this approach.

In a case of a free inlet of a sub-critical flow, i.e. when the water level in the junction is lower than the critical depth level in the inlet link, the water level in the link is assumed to be equal to the critical depth. For different cross sections, appropriate approximations are applied, e.g. for a circular pipe as follows:

$$y_{c(i)} = \sqrt{0.32\frac{Q_i}{\sqrt{D_i}}}$$

(7.13)

where:

D_i=diameter of the circular pipe [m].

Similarly, in a case of a low water level in the junction with supercritical flow (steep inlet links), the downstream water level is set equal to normal depth in the link.

7.3.2 Head losses at the outlet from a node

All the individual losses in a node (except the inlet loss) calculated by the model are added-up at the outlet, separately for each outlet link. The outlet

loss for the link j is assumed to be proportional to the velocity head in the outlet link j:

$$\Delta E_j = \sum_k \zeta_{jk} \cdot \frac{v_j^2}{2g} \qquad (7.14)$$

where ξ_{jk} are individual head loss coefficients for link j, calculated on the basis of geometrical set-up of the node and flow distribution among the links attached to the node.

The model distinguishes among the following losses:

- Change in flow direction,

- Change in elevation,

- Loss due to contraction at outlet.

Loss due to change in flow direction

This loss is a function of the angles between the inlet and outlet links and distribution of the discharge in the inlet and outlet links, as shown in Figure 7.3 and Figure 7.4.
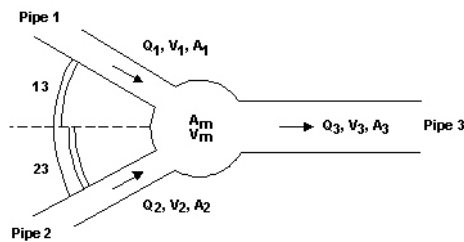

Figure 7.3   Manhole consisting of 2 inlet links and 1 outlet link
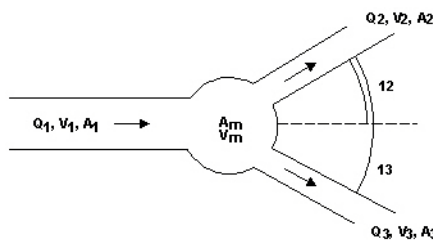
Figure 7.4   Manhole consisting of 1 inlet link and 2 outlet links

Based on the generalised notation, the calculation of the head loss coefficient is performed individually for each outlet link as follows:

$$\zeta_{dir(j)} = \sum_{i=1}^{n} \frac{Q_i}{Q_j} \cdot \frac{\theta_{ij}^2}{90°^2} \qquad (7.15)$$

where i stands for inlet links, and j stands for outlet links.

Loss Due to Change in Elevation

Vertical changes in flow direction occur and cause energy losses if there is a difference in elevation between inlet and outlet link. These losses are described considering the magnitude of the difference in elevation, see Figure 7.5.
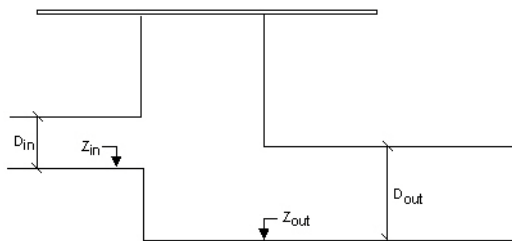
Figure 7.5   Manhole with a difference in elevation between inlet and outlet pipe

The individual head loss coefficient is calculated according to the following expression, where the weighting relative to the flow rates in the inlet links relative to the outlet link is also included:

$$\zeta_{level(j)} = \sum_{i=1}^{n} \frac{Q_i}{Q_j} \cdot \frac{(Z_j - Z_i) \cdot (Z_j + D_j - Z_i - D_i)}{D_i \cdot D_j} \qquad (7.16)$$

If the calculated head loss coefficient is smaller than 0, a zero value is assumed.

Loss Due to Contraction

The flow leaving the manhole and entering the outlet conduit is more or less contracted and due to subsequent expansion there occurs an energy loss. The outlet head loss coefficient depends on the shape of the manhole outlet, manhole and the link cross sections and distribution of flow among multiple inlet and outlet links.

MOUSE calculates the outlet head loss coefficient according to the following:

$$\zeta_{contr(j)} = K_m \cdot \left| 1 - \frac{A_j}{A_m \cdot \dfrac{Q_j}{\displaystyle\sum_{i=1}^{n} Q_i}} \right| \qquad (7.17)$$

where:

K_m	=	specified outlet 'shape' coefficient for the node. For relatively large basins, K_m approaches ζ_{contr}.
A_m	=	flow cross sectional area in the node.

7.3.3 Implementation of the Total Energy Loss Computation

Theoretically, the total energy loss at the outlet from the node, expressed as a function of the velocity head in the outlet pipe can be as high as the available energy level in the node. The limiting case occurs e.g. with completely clogged outlet ($K_m \to \infty$), with no flow in the outlet pipe.

However, in computational reality, in order to preserve a robustness of the computation, various additional limitations could be introduced. With respect to that, MOUSE offers two possibilities.

The first limitation relates the maximum head loss to the depth in the outlet pipe:

$$\Delta h_j = \min \left[h_j, \left((1 + \zeta_{out}) \cdot \frac{v_j^2}{2g} - \frac{v_m^2}{2g} \right) \right] \qquad (7.18)$$

It also introduces the limitation on the total head loss coefficient as:

$$\zeta_{out} = \Sigma \zeta_j \leq 1.0 \qquad (7.19)$$

These limitations have caused that the computed head losses and the corresponding flow conditions around nodes in some cases were inexact.

Due to the advances in the computational implementation, the limitation from Equation (7.19) could been removed, allowing the total energy loss for the outlet pipe j being computed as:

$$\Delta E_j = \min[\zeta_{dir(j)} + \zeta_{level(j)} + \zeta_{contr(j)}, 1] \cdot \frac{v_j^2}{2g} \tag{7.20}$$

The limitation of the total head loss coefficient to 1.0 is, however, still present.

7.4 An Alternative Solution Based on Weighted Inlet Energy Levels

The assumption applied in the MOUSE 'standard' solution that the water level in the manhole and all downstream water levels of the inflowing conduits are the same, often leads to overestimates of the energy loss at the inlet. In many cases, the wetted cross-section area in the inlet pipe is smaller than in the manhole, leading to almost entire loss of the kinetic energy of the incoming flows, which is not the case. This problem is reduced by applying the effective flow area in the manhole, but this is available in MOUSE only for circular pipes and for the flow-through manholes (i.e. with one pipe in- and one pipe outflow).

An alternative solution is available which fully ignores the energy loss at the inlet. For a flow-through manhole, this practically means that the energy level in the manhole is set to be equal as at the downstream end of the inlet pipe. For manholes with multiple inlets, the energy level is calculated as the weighted average of the inlet flows (i.e. large flows contribute most to the energy level).

Thus, in this formulation, the total loss at the manhole is concentrated computationally at the outlet, and can be fully controlled by the user.

Without doubt, this approach proves valuable for some specific situations, particularly for the flow-through manholes with 'normal' flow conditions. However, due attention must be paid for cases with high inlet energy levels, e.g. a small pipe with high-velocity flow entering a large basin. In such a case, the energy level of otherwise still water in the basin would be calculated as equal to the energy level of the approaching flow, i.e. much higher than realistic, with erroneous results as a consequence.

7.5 Selecting an Appropriate Local Head-loss Computation

In some cases, results from using different approach for node head loss calculation can be considerably different, and due attention must be paid to the selection of the most appropriate approach.

The head loss calculation for individual nodes can be controlled by selecting one of the available options - there are default five options in MIKE URBAN. You can always create your own option.

Each option is characterised by the fundamental computational principle and by a number of parameters which control the behaviour of the algorithm or the size of loss coefficient. In MIKE URBAN, the existing options can be modified and new options created in "Outlet Head Loss" dialog. Furthermore, the actual head loss calculation for individual nodes can be both in MOUSE and in MIKE URBAN controlled by a local specification of various relevant parameters.

7.5.1 Constitutive Parameters of Head Loss Computation Options

The following parameters constitute a definition of head loss calculation option:

Computation Method

Three different methods are avialable:

- MOUSE Classic (Engelund) - described in section 7.3
- Weighted Inlet Energy Method - described in section 7.4
- No Head Loss Calculation

The first two are described in detail in respective chapters.

The third option ignores all local losses. Regardless of the shape of the outlets, geometrical set-up of the junction and distribution of flows among inlet and outlet conduits, water levels in the junction and the outlet conduit are set equal, as if there is no change of geometry and the flow conditions between the junction and outlet conduit. This literary means that this option should be applied only where there is no change in cross section. If inappropriately applied, inconsistent results may be generated.

On the contrary, this option can be recommended for use if an artificial node is introduced somewhere on a straight section of a conduit, where actually no losses occur.

Maximum Loss Limit

This parameter is of relevance for both MOUSE Classic and Weigthed Inlet Energy computation methods. It actually sets the limitation on the maximum computed headloss to the water depth or the velocity head in the outlet pipe, according to equations (7.18) to (7.20).

Loss Coefficient

The available loss coefficient types distinguish three different interpretations of the specified head loss coefficient.

Selection of "K$_m$ " (Type (a)) interprets the specified value as the outlet 'shape' coefficient *Km* (see Equation (7.17)).

Selection of "Contraction HLC" (Type (b)) interprets the specified value as the outlet 'contraction' coefficient *zcontr(j)* (see Equation (7.17)). This means that the model ignores the geometrical relations between the node and the outlet links (outlet shape), and applies the specified value directly as the *zcontr*. The contraction losses in the outlet links are then computed by multiplying the velocity head in the respective link by the *zcontr*. The total head loss for an outlet link is computed as a sum of the contraction, direction and elevation loss.

Selection of "Total HLC" (Type c)) interprets the specified value as the total outlet head loss. This means that the model completely ignores the geometry of the node/links, and applies the specified value (Total HLC) directly as the z_{out}, the same for all outlet links at the node. The total head losses in the outlet links are then computed by multiplying the velocity head in the respective link by the specified z_{out}.

Effective Node Area

This parameter is only relevant for MOUSE classic computational method and for flow-through manholes in circular pipes. In all other cases, the default total wetted node area is applied. The following choices are available:

Total wetted area: calculated as product of diameter and water depth for manholes and red from the basin geometry table (A_c) for basins. Typically results in overestimate of local loss in a node.

Calculated Effective Area: The effective area in a manhole is calculated on the basis of empirical formula (see section 2.3.2 Types and Definition of Nodes *(p. 19)*). This results in a significantly smaller area than full wetted area and, consequently with a more realistic flow calculation.

Reduced Calculated Effective Area: The effective area in a manhole is further reduced to 50% of the calculated effective area.

7.5.2   Default Computational Options

The following tables provide an overview of available head loss calculation options in MIKE URBAN.

MIKE URBAN DEFAULT OPTIONS	Method	Loss Limit	Coefficient Type	Coeff.	Effective Node Area
MOUSE Classic (Engelund)	Classic	Water depth	Km	0.25	Full
MOUSE Classic (Engelund)-Modified	Classic	Velocity head	Km	0.25	Full
Flow Through Manhole	Classic	Water depth	Km	0.25	Calculated
No Cross Section Changes	No head loss calculation	n/a	n/a	0	n/a
Weighted Inlet Energy	Weighted Inlet Energy	Water depth	Km	0.25	Full

7.5.3 Example: Node Outlet Head Losses Variation as Function of Head Loss Coefficient Mode

In this example a simple sewer system consisting of two pipes, two manholes and one outlet is constructed. Tests for different head-loss types (a), (b) and (c) have been performed with various modifications in flow direction or drop height, or both. Table 7.1 shows a complete test matrix.

Four variants of the model setup have been constructed:

I)Straight sewer pipelines with no drops and no changes in directions.

II)A change in direction is introduced in variant I).

III)A drop is introduced in variant I).

IV)A drop and a change in direction are introduced in variant I).

A definition sketch of the setups I)-IV) is shown in Figure 7.6. The manual calculation example corresponds to test No. 4 in the test matrix.
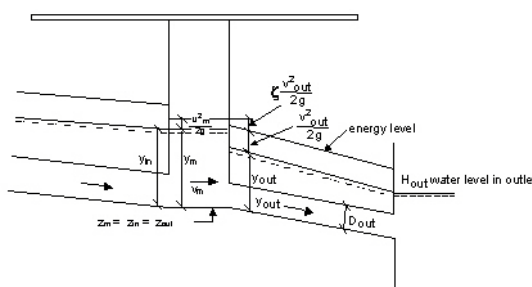

Figure 7.6   Example definition sketch

In the performed tests, the value of the HEADLOSS COEFFICIENT has been set to 0.5 for all three types (a), (b) and (c). The head loss coefficients for drop in the setup III) and IV) is 0.4 (inlet pipe is 0.6 m above the bottom in manhole B). The head loss for direction in the setup II) and IV) is 0.25 (angle between pipes are 45°).

The example also includes calculation of the friction loss in the downstream pipe.

Manual Head Loss Calculation

Assumptions:

The water level in the inlet pipe is assumed equal to the water level in the manhole. This implies that the expansion loss at the inlet is automatically assumed. All calculated energy losses are assumed to occur at the outlet pipe, i.e.:

$$E_{manhole} = E_{pipe} + \Delta H \tag{7.21}$$

or expressed by using the notation in Figure 7.6:

$$\frac{v_m^2}{2g} + y_m + Z_m = \frac{v_{out}^2}{2g} + y_{out} + Z_{out} + \zeta \frac{v_{out}^2}{2g} \tag{7.22}$$

ζ = a coefficient expressing the total outlet energy loss (see section 7.3.2 Head losses at the outlet from a node *(p. 89)*).

Data:

Discharge	Q	=	2.0	m³s⁻¹
Diameter in outlet pipe	D_{out}	=	1.0	m
Diameter in manhole	D_m	=	1.5	m
Velocity in outlet pipe (Q is capacity assumed)	V_{out}	~	2.55	ms⁻¹
Length of outlet pipe	L	=	50.0	m
Manning number	M	=	70	m¹ᐟ³s⁻¹
Water level in outlet	H_{out}	=	15.0	m
Bottom level in manhole	Z_m	=	14.0	m
Head "shape" loss coefficient	K_m	=	0.5	

Friction loss in outlet pipe from manhole to outlet:

$$h_f = \frac{Q^2 L}{M^2 A^2 R^{4/3}} = \frac{2.0^2 \cdot 50.0}{70^2 \cdot 0.7854^2 \cdot 0.25^{4/3}} \tag{7.23}$$

The water level in the manhole (*H*) can be found from:

$$H + \frac{v_m^2}{2g} = H_{out} + h_f + \frac{v_{out}^2}{2g} + \zeta \frac{v_{out}^2}{2g} \tag{7.24}$$

v_m is approximated by assuming that $y_m = y_{out}$:

$$v_m = \frac{Q}{A_m} = \frac{Q}{D_m y_m} = \frac{2.0}{1.5 \cdot (15.0 + 0.42 - 14.0)} = 0.94 ms^{-1} \qquad (7.25)$$

$$v_{out} = \frac{Q}{A_{out}} = \frac{2.0}{0.78} = 2.55 ms^{-1}, \quad \frac{v_{out}^2}{2g} = 0.33 m \qquad (7.26)$$

$$\frac{v_m^2}{2g} = 0.045 \text{ m} \qquad (7.27)$$

$$\zeta = \zeta_{contr} + \zeta_{dir} \qquad (7.28)$$

$$= K_m \cdot (1 - \frac{A_{out}}{Q_{out}} \frac{Q_{in}}{A_m}) + \frac{Q_{in}}{Q_{out}} \cdot \frac{\theta^2}{90^2}$$

$$= (1 - \frac{0.78}{1.5 \cdot 1.42}) + \frac{45^2}{90^2} = 0.567$$

Substituting values to the Equation (7.25) and calculating H yields:

$$H = 15.89 \text{ m} \qquad (7.29)$$

The deviation between the MOUSE simulation and manual calculation result is due to the fact that MOUSE calculates v_{out} by using the following area in the pipe:

$$A_{out} = \frac{D_{out}^2 \pi}{4} + \text{Preismann slot area}$$

The table shows which setups have been used for the calculation, and also which head loss types are included. ζ_{c0}, ζ_{c1}, ζ_{c2} are all head loss coefficients due to contraction and correspond to the types (a) , (b) and (c).

Table 7.1   Test matrix for implementation fo Head Loss Type

Table 7.2

Test	Setup	Direction ζ_d	Drop ζ_l	Contraction ζ_c			H_{calc}	H_M
				(a) ζ_{c0}	(b)ζ_{c1}	(c)ζ_{c0}		
1	I)			X			15.81	15.82
2	I)				X		15.87	15.87
3	I)					X	15.87	15.87

Table 7.2

Test	Setup	Direction ζ_d	Drop ζ_l	Contraction ζ_c			H_{calc}	H_M
				(a) ζ_{c0}	(b) ζ_{c1}	(c) ζ_{c0}		
4	II)	X		X			15.89	15.90
5	II)	X			X		15.95	15.94
6	II)	X				X	15.87	15.87
7	III)		X	X			15.94	15.94
8	III)		X		X		16.00	15.99
9	IV)	X	X	X			16.02	16.02
10	IV)	X	X		X		16.03	16.02

7.5.4 Implementation of Head Loss Description in Kinematic Wave Simulations

When applying the kinematic wave approximation, the head loss description in nodes is based on the same equations as described above.

However, in order to reduce the computational time, the energy losses are computed once for a number of different flow conditions and tabulated for use during the simulation. In cases where there is more than one inlet link in a manhole, the losses are calculated on the basis of the assumption that the flow in each link (relative to the flow in the other inlet links) is proportional to the corresponding full flow capacity. This assumption affects the energy losses due to changes in elevation and direction only when these losses are different for the different inlet links.

8 Some Special Techniques

8.1 Surface Flooding

If the water level in a manhole or a basin reaches the ground level, an artificial "inundation" basin is inserted above the node. The surface area of this basin is gradually (over one meter) increased from the area in the manhole or the basin to a 1000 times larger area, thus simulating the surface inundation. The maximum level of inundation is 10 meter above the specified ground level. When the outflow from the node surmounts the inflow, the water stored in the inundation basin re-enters the system.

When the water level in the node increases and is above ground level, the following is assumed:

During a time step the surface area in the basin is calculated using the water level from the start of the actual time step. A situation like this is shown in Figure 8.1. If the water level passes through the transition region between the actual manhole or structure and the artificial basin, this assumption leads to generation of water. In Figure 8.1 the shaded area illustrates the generated volume of water.
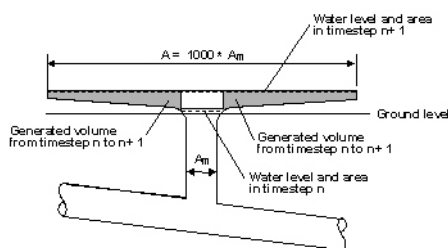

Figure 8.1   Simulation of the surface flooding

When the increase of the water level during a time step is relatively small, then the generated water volume is negligible. If the water level is changing rapidly, the generated volume of water is important and due to that an appropriate correction is built in the program to ensure no generation of water.

An alternative to the assumption of constant surface area during a time step is to introduce iterations in the simulation. Iterations would significantly increase the simulation time.

8.2 Sealed Nodes

Any manhole or basin can be defined as 'sealed'. If a node is defined as a sealed node, then the maximum water level at a node is set to the ground

surface. In this case, the pressure will rise without any water on the ground surface. The following relations are valid:

$$H_m = P_m \text{ for } P_m \le H_{top} \tag{8.1}$$
$$and$$
$$H_m = H_{top} \text{ for } P_m > H_{top}$$

where:

H_m is the water level in the node [m],
P_m is the pressure level in the node [m],
H_{top} is the ground level for the node [m].

8.3   Spilling Nodes

Any manhole or basin can be defined as 'spilling'. If the water level in a node defined as a spilling node reaches the ground level, the water will start spilling irreversibly out of the system. The flow will be computed using the free over-flow formula, according to the following:

$$\text{for } H_m \le (H_{top} + \Delta P): \tag{8.2}$$
$$Q_{spill} = 0;$$

$$\text{for } H_m > (H_{top} + \Delta P):$$
$$Q_{spill} = \text{Relative Weir Coefficient} \cdot 0.63 \cdot B \cdot \sqrt{2g} \cdot (H_m - (H_{top} + \Delta P))^{3/2}$$

where:

Q_{spill} =   the spill discharge [m³/s],
B =   a conceptual spill width [m],
H_m =   the water level in the manhole [m],
H_{top} =   the ground level in the manhole [m],
ΔP =   the "Buffer Pressure Level" for the spill [m],
g =   the acceleration of gravity [ms⁻²],
RelativeWeirCoefficient = the linear scaling coefficient for the spill.

The level (i.e. head) at which the spill starts can be controlled by optionally specifying the 'Buffer Pressure Level' as a relative elevation above (or below) the ground surface (default value = 0).

For circular manholes, the spill width B equals to 1.5 times the manhole diameter for the water level $H_m = H_{top}+\Delta P$. With increasing water level, the spill width B increases, following the same functional relation as used for the "basin" area above surcharging nodes (i.e. increases exponentially to approximately max. 1000 times the manhole diameter) - see paragraph 8.1. For

nodes defined as basins, the spill width *B* is set equal to the square root of the basin surface area.

The spilling capacity of a spilling manhole can be controlled by specifying the Relative Weir Coefficient (default value = 1).

8.4   Pressure Mains

The 'pressure mains' (also referred to as rising mains in earlier versions of MOUSE) feature is intended for modeling the permanently pressurized individual pipes or networks in connection to pumps. Computationally MOUSE assumes that a rising main network always runs under pressure and therefore the reaction time within the rising main network is insignificant.

Solution in pressure mains is based on the two equations:

$$\frac{\partial Q}{\partial x} = 0 \tag{8.3}$$

and

$$\frac{\partial Q}{\partial t} + gA\frac{\partial y}{\partial x} = gA(I_0 - I_f) \tag{8.4}$$

where

Q	=	discharge, [m³s⁻¹]
A	=	flow area, [m²]
y	=	flow depth, [m]
g	=	acceleration of gravity, [ms⁻²]
x	=	distance in the flow direction, [m]
t	=	time, [s]
I_0	=	bottom slope
I_f	=	friction slope

All nodes within the pressure main networks are assumed to be sealed.

MOUSE supports modeling of an arbitrary number of pressure main networks and there is no limitation on the number of elements in each sub network.

Pressure main networks must always converge down to one receiving manhole, which is called the tail node. The tail node is the point of transition between domains where the hydraulic solution is based on the St. Venant equation and the special pressure main model.

The computation of the special pressure main sub models uses the maximum of the water level in the "St Venant" governed domain and the water level at the tail nodes as downstream boundary conditions. As default it is assumed

that the tail node water level is equal to the maximum of the up-vert level of all pressure pipes attached to the tail node, but the user can change this default value.

The "upstream" pressure main network must be linked with the St. Venant controlled domain through pumps. The "pressure mains" feature can handle an unlimited number of pumps attached to one pressure main network, but the solution feature can only handle networks where the upstream link to the St Venant domain is modeled by pumps.

8.5   Dry Conduits

If parts of the sewer system dry-out during the simulation, then the model artificially maintains a minimum water depth in those conduits, corresponding (per default) to 5‰ of the characteristic dimension of the conduit (diameter for circular pipes), or max. 5 mm. This is necessary with regards to the numerical stability in the solution of the flow equations.

This correction practically means artificial generation of water, i.e. some water volume is added to the system. As a consequence of that, the continuity status report shown at the end of the simulation does not give a fair impression of the accuracy of the simulation.

8.6   A note on flooding and spilling

The term "flooding" is used when water level is above ground level, and "floodrate" is the volume of water per second running from below ground level to above ground level.

Spilling is defined when water is running out of the system and "spilling rate" is the volume of water per second running out of the system.

Flooding, floodrate, spilling, and spilling rate can all be reported in an .XRF-file for MOUSE and in the .AddOut.res1d-file for MIKE 1D.

Note that floodrate can be both positive (water coming from below ground level) and negative (water running into the ground level), while spilling rate can only be positive.

Since both nodes and pipes can have Preismann slots that emulate pressurized nodes or pipes, it often happens that there is flooding in the system but NOT spilling. Thus, flooding does not necessarily mean that there is water running out of the system onto the ground.

Water volume above ground level in nodes is calculated as total water volume on the node minus water volume below ground level. This means that sealed nodes can also have some (small) amount of flooding due to the slot which extends above ground level.

Spilling nodes have two input parameters - buffer pressure and spilling coefficient. The buffer pressure represents the water depth above ground needed before water is lost from the system. Hence, if you set the buffer pressure to e.g. 10 cm then water will not spill before the water level is more than 10 cm above ground level. In this case you will also see flooding because water is between ground level and ground level + 10 cm, but it is not lost from the system. Hence when the water level is reduced this volume of water is going back into the network again. Hence some water is flooding and going back to the network again while another volume is spilled and lost to the system.

The buffer pressure is used to model the effect of two physical processes: 1) a cover that requires a certain pressure before it lifts and water is lost (in this case the water level above ground is really a pressure and hence no real water is on the ground), and 2) a sewer grate that is located in a small depression in the road and it is not until the water level is above 10 cm that water starts running down the street and is lost to the system (in this case there actually is water on the ground even though it is not lost.)

When the buffer pressure is zero, the spilling coefficient is still used. Spilling is calculated as water spilling over a weir. The weir coefficient is equal to the spilling coefficient and the weir width is calculated from the circumference of the manhole. In some cases the spilling weir becomes a restriction on the flow and then the water level will build up behind the weir (i.e. in the manhole itself) and the water level will become higher than the ground. Also this is reported as flooding, because the water level is above ground level.

9   Nomenclature

a,b,c,..,z quasi-constants in a modified continuity equation around a node

A,*B*,..,*Z* quasi-constants in a generalised continuity equation around a
node

a the speed of sound in water, with actual pipe walls rigidity, (ms^{-1})

a vertical distance from the point where the jet intercepts the manhole to the centreline of the inlet

a_o the speed of sound in water for absolutely rigid pipe walls, (ms^{-1})

a_r the speed of sound along pipe walls, (ms^{-1})

A cross-section area, (m^2)

A_{flow} effective flow area in a manhole, (m^2)

A_{jet} crosssection area of the jet at the point of interception with the manhole, (m^2)

A_m crosssection area of the wet part of the manhole, (m^2)

A_{full} cross-section area at full pipe flow, (m^2)

A_o the cross-section area without excess pressure, (m^2)

A_t structure, wetted cross section area, (m^2)

A_0 structure, water surface area, (m^2)

$A_{0,j}$ surface area between grid points *j-1* and *j*

$A_{0,j+1}$ surface area between grid points *j* and *j+1*

b vertical distance from the point where the side of the outlet enters the manhole to the centreline of the inlet

b surface width, (m)

b_s storage width, (m)

b_{slot} width of Preissmann slot, (m)

B overflows, width, (m)

$C = AR^{2/3}$ cross-section conveyance, ($m^{8/3}$)

C_r Courant number

C_d Coefficient of discharge

C_E Coefficient of discharge (energy based)

C_H Coefficient of discharge (level based)

D pipe diameter, (m)

D_{in} diameter of the inlet pipe, (m)

D_m diameter of the manhole, (m)

D_{out} diameter of the outlet pipe, (m)

$drop\_ factor$ factor diminishing the effective flow area in a manhole due to
drop in elevation

e the pipe wall thickness, (m)

E energy level just upstream overflow (m)

exp Manning's number variation exponent, default 1.00

E_r the Young's modulus of elasticity, (Nm^{-2})

f coeff. for flow direction change (default $f =1$)

$g = 9.81$ constant, acceleration of gravity, (ms^{-2})

Fr Froude's number

h water level, (m)

H cross sections - elevation relative to bottom, (m) pumps, water level in a pump-sump, (m) overflows, water level just upstream the overflow, (m)

ΔH overflows, entrance energy loss, (m) pumps, level difference between two nodes

H_A regulation, water level at the control point A, (m)

H_{bott} node, bottom elevation, (m)

H_m water level in a node, (m)

$H_{min},$

H_{max}regulation, water levels at the control point *A* defining the range in which the regulation is to be applied, (m)

H_{out}water surface elevation at outlet, (m)

H_{start},

H_{stop}pumps, start and stop level for a pump, (m)

H_{top}node, surface elevation, (m)

H_{up},H_{down} or

H_1,H_2water levels at the computational points upstream and down stream, respectively, (m)

I_0bottom slope, (m^{-1})

$I_f$friction slope, (m^{-1})

$k$wall roughness (m)

$K_c$overflows, energy loss coefficient

$K_m$specified outlet 'shape' coefficient for a node

*l*conduit length, (m)

$l_r$pipe length which gives rise to pressurised flow, (m)

*M*Manning number, (m$^{1/3}$s^{-1})

M_{act}calculated Manning's number, (m$^{1/3}$s^{-1})

M_{bott}Manning's numbers specified for the conduit bottom, (m$^{1/3}$s^{-1})

M_{full}Manning number at full pipe flow, (m$^{1/3}$s^{-1})

*n*invers of manning number (*1/M*)

*N*number of grid points in a pipe

*q*specific discharge, (m^{2}s^{-1})

*Q*discharge, (m^{3}s^{-1})

Q_{full}full pipe flow for uniform flow conditions, (m^{3}s^{-1})

$Q(H_A)$regulation, discharge defined by the regulation function, (m^{3}s^{-1})

Q_{nat}regulation, "natural" discharge, (m^{3}s^{-1})

Q_{reg} regulation, applied discharge, (m^3s^{-1})

Q_{weir} overflows, discharge, (m^3s^{-1})

$R = A/P$ hydraulic radius, (m)

R_{full} hydraulic radius at full pipe flow, (m)

t time, (s)

Δt computational time step, (s)

v mean flow velocity, (ms^{-1})

v_m flow velocity in a node, (ms^{-1})

w_0 gate opening

w_1 distance from the overflow crest to the upstream bottom (m)

w_2 distance from the overflow crest to the downstream bottom (m)

x distance in the flow direction, (m)

Δx distance between two computational points, (m)

x,y node co-ordinates, (m)

y depth, (m)

y depth in a contracted section (m)

$y_1 \ y_2 \ y_3$ depth in upstream, central and downstream section, (m)

y_c critical depth, (m)

y_n normal (natural) depth, (m)

y/D the relative water depth

Z generalised flow variable, substituting h and Q

α Coriolis' velocity distribution coefficient

$\alpha, \beta, \gamma, \delta$ coefficients in finite-difference equations

$\zeta_{(j)}$ total calculated node head loss coefficient for outlet conduit j

ζ_{dir} calculated node head loss coefficient, due to change of direction

$\zeta_{elevation}$ calculated node head loss coefficient, due to change of elevation

$\zeta_{contr(j)}$calculated outlet contraction head loss coefficient, for outlet conduit j

θweighting coefficent of the numerical scheme

θ_{ij}horizontal angle between inlet conduit i and outlet conduit j

ρwater density, (kgm^{-3})

$\rho_o$density of water for a free surface flow, (kgm^{-3})

τtangential stress caused by the wall friction, (Nm^{-2})

υkinematic viscosity (m^{2}s^{-1})

$\psi_v$vertical contraction coeff.

10 References

/1/ MOUSE User Manual and Tutorial, DHI 1999

/2/ Abbott, M.B.: Computational Hydraulics, Elements of the Theory of Free Surface Flows, Pitman, 1979.

/3/ Pedersen, F.B., Mark, O.: Head Losses in Storm Sewer Manholes: Submerged Jet Theory, Journal of Hydraulic Engineering, Vol. 116, No. 11, November 1990.

/4/ Cunge J.A. and Wegner M. (1964): Integration numerique des equations d'ecoulement de Barre de Saint-Venant par un schema implicite de differences finies: Application au cas d'une galerie tantot en charge, tantot a surface libre. La Houille Blance, No 1

/5/ F.A. Engelund og Fl. Bo Pedersen: Hydraulik, Den Private Ingeniørfond, Danmarks Tekniske Højskole, ISBN 87-87245-64-7 (In Danish)